Quantum electronics

中央研究院物理研究所　陳啟東

e-mail: chiidong@phys.sinica.edu.tw
網址：　http://www.phys.sinica.edu.tw/~quela

Outline:

Device fabrication

- **e-beam lithography, examples**

Measurement electronics

Electron transport in

- **Ballistic systems**
- **Highly disordered systems**

Hopping conduction in diluted trap systems

- **Tunneling through quantum dots**

} **metal to insulator transition**

Quantum bits:

- **Resonant tunneling between coupled quantum-dots**
- **from small Josephson junctions to charge qubits**

State-of-the-art mass-production technology

45nm node

high K
gate oxide

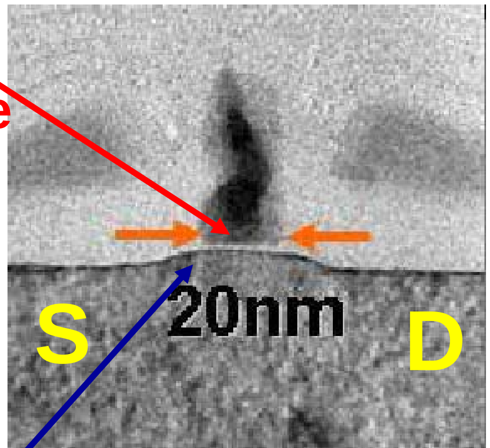

strained
channel

45 nm process
2009 production

32nm node

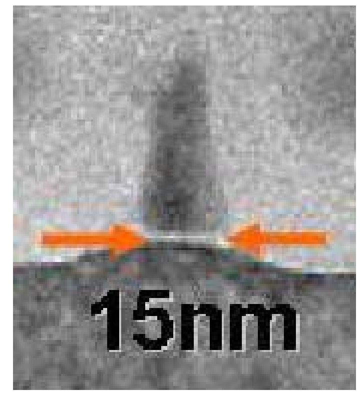

32 nm process
2009 production

Light source = 193 nm Argon Fluoride excimer laser

But for research purpose, we use focused electron beam sources

Mix and Match technology

Photolithography

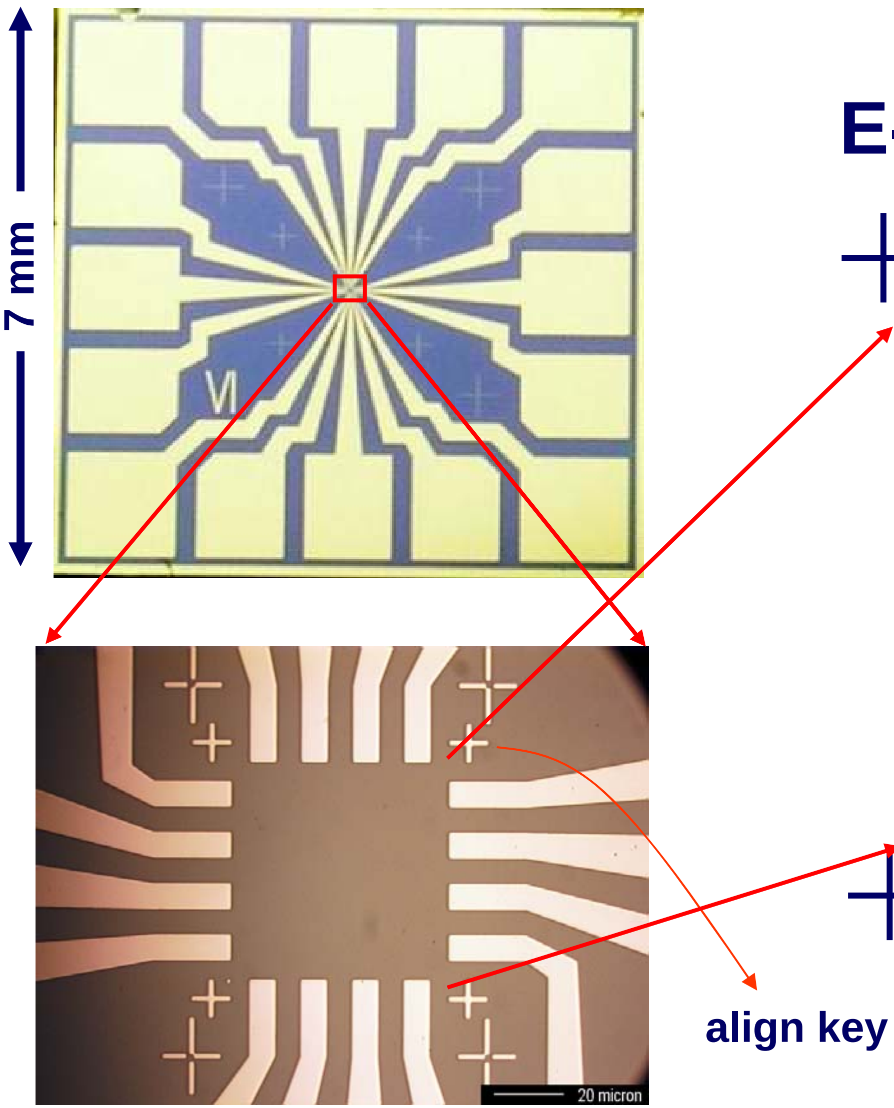

E-beam lithography

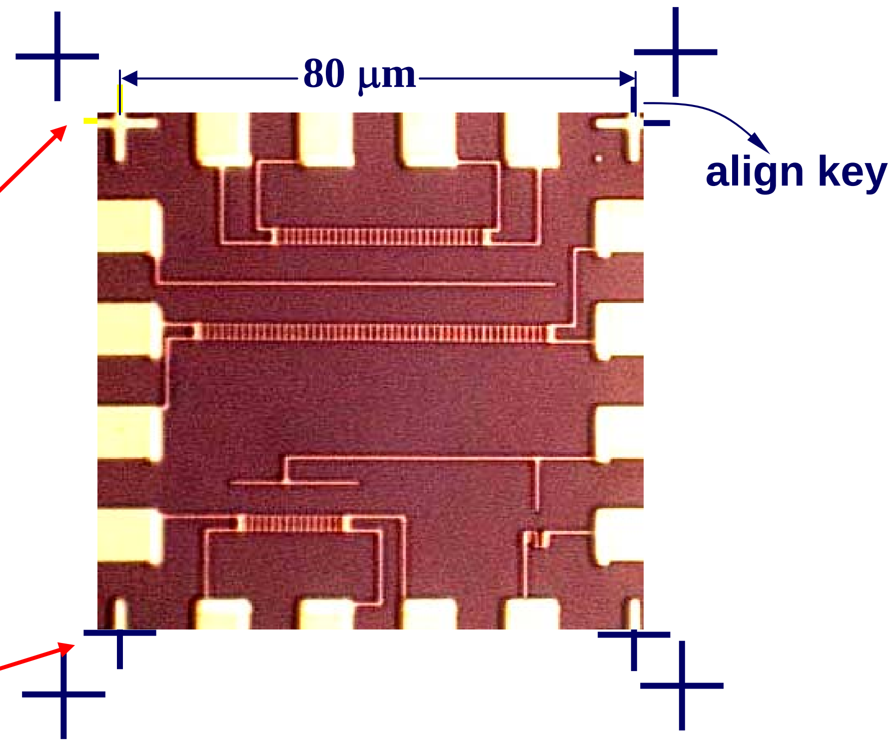

Electron beam lithography
and lift-off technique

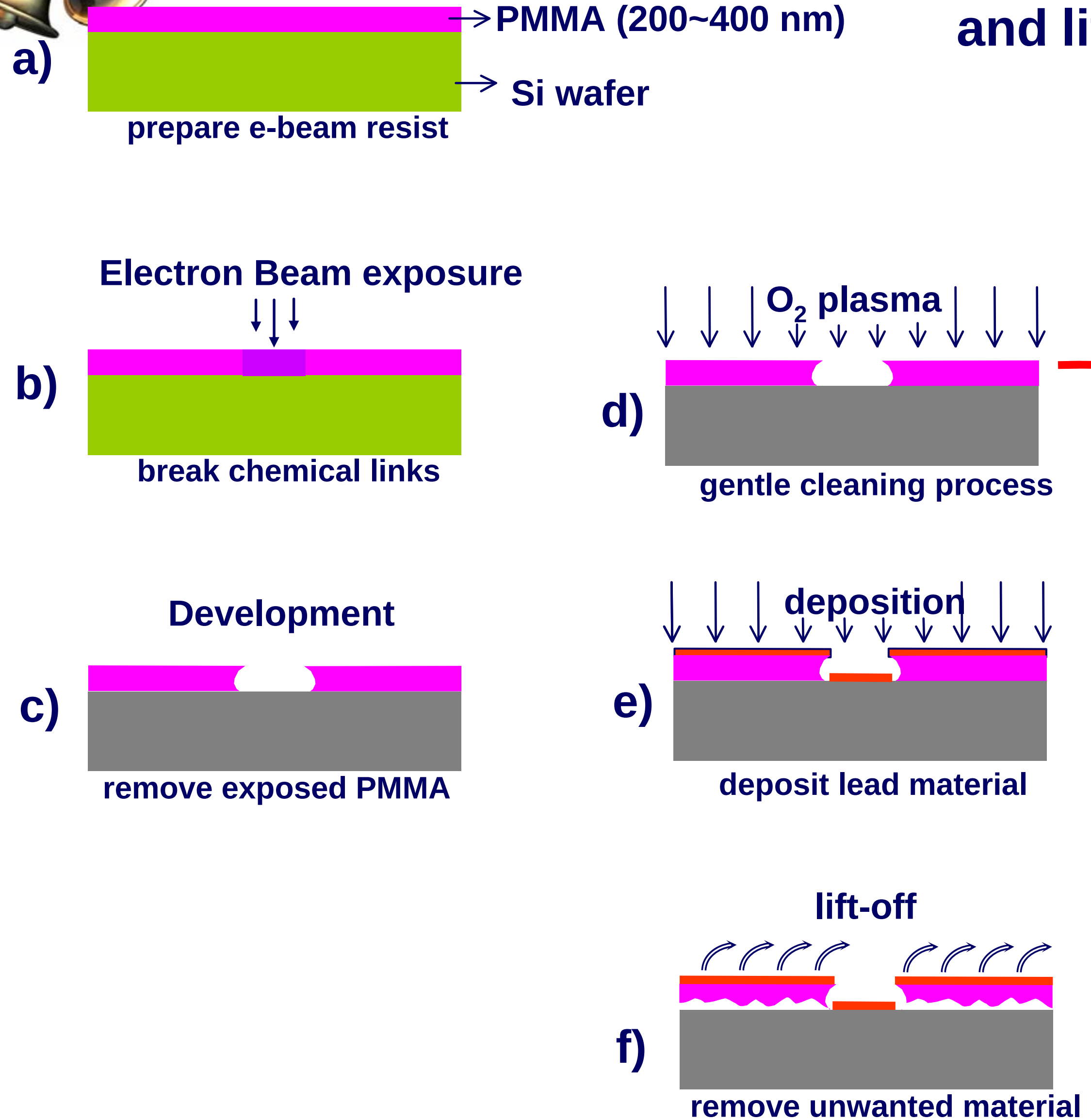

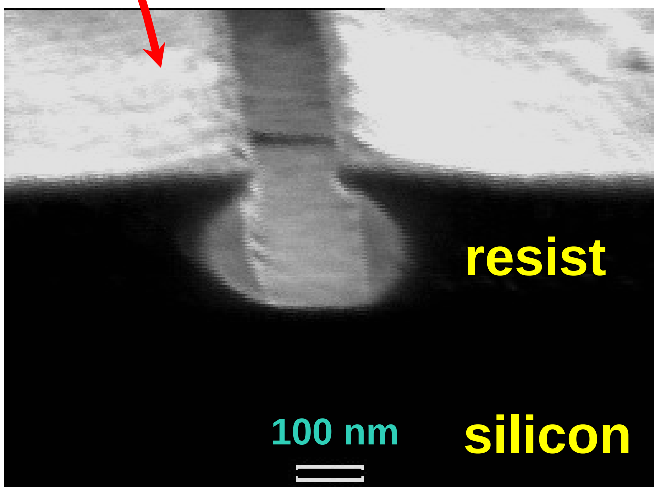

Resist profile engineering:
Fabrication of Aluminum tunnel junctions

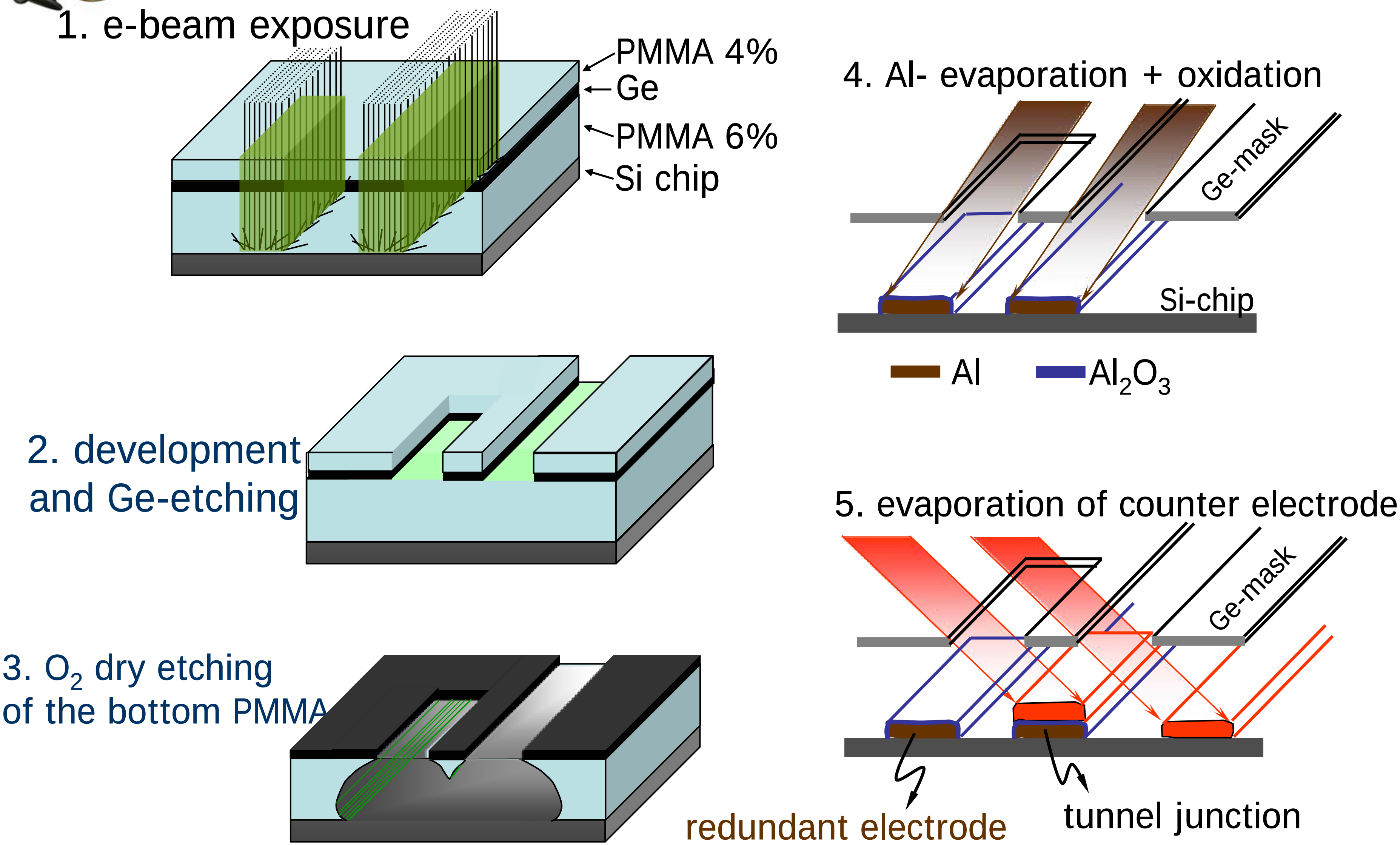

Multiple angle evaporations

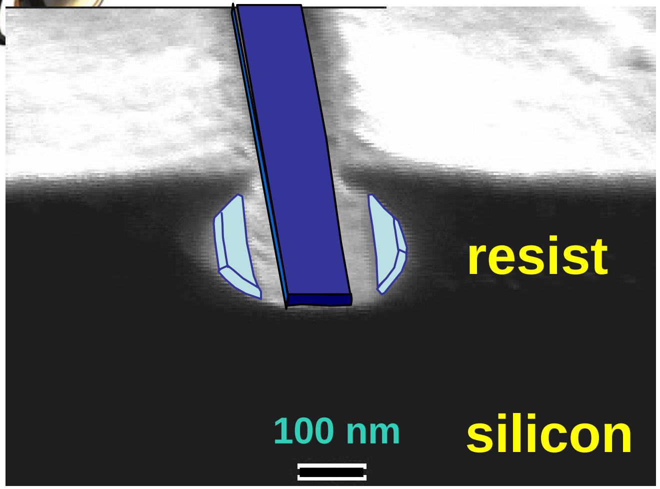

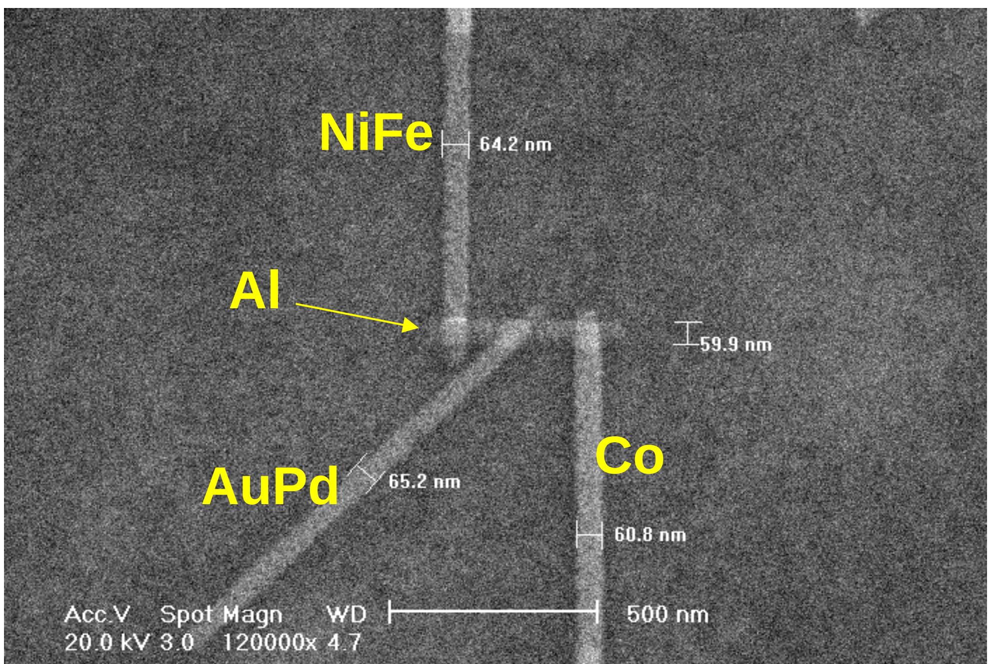

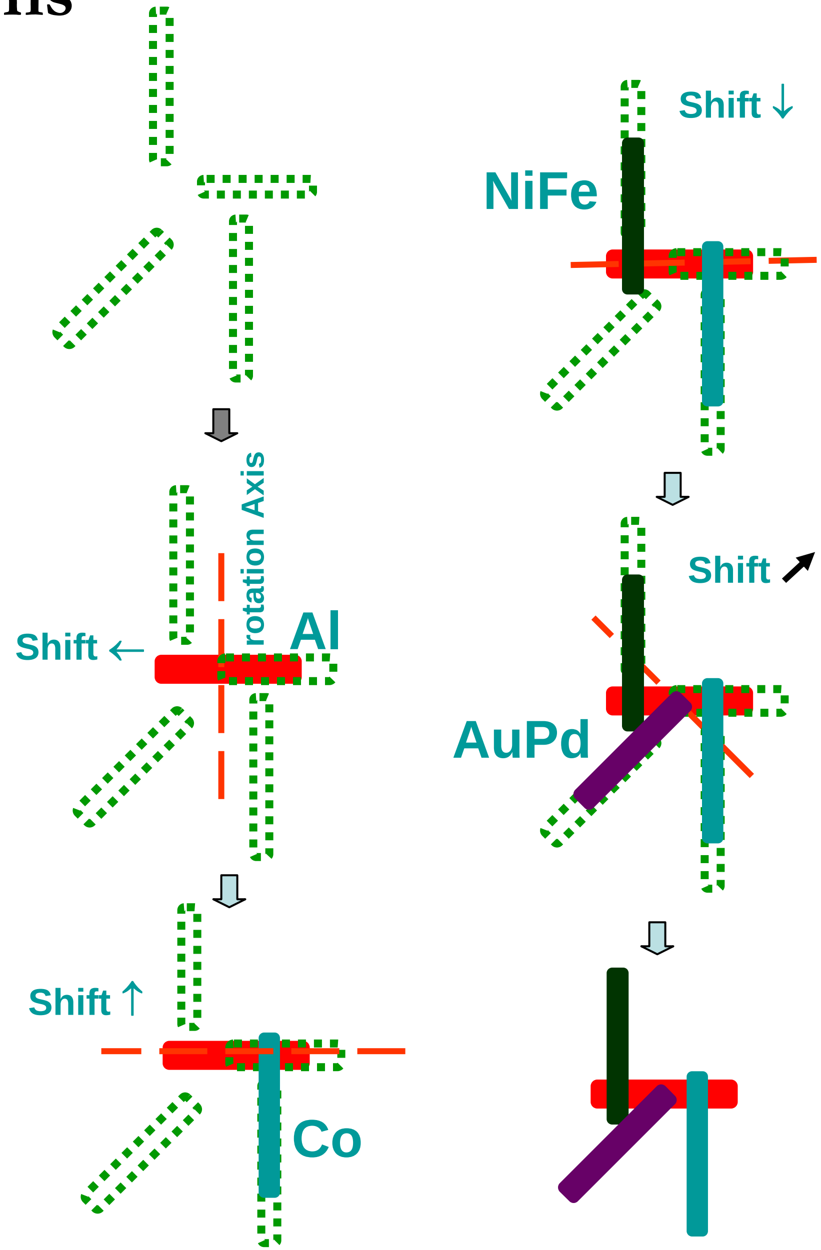

Metallic electronics

Single electron devices

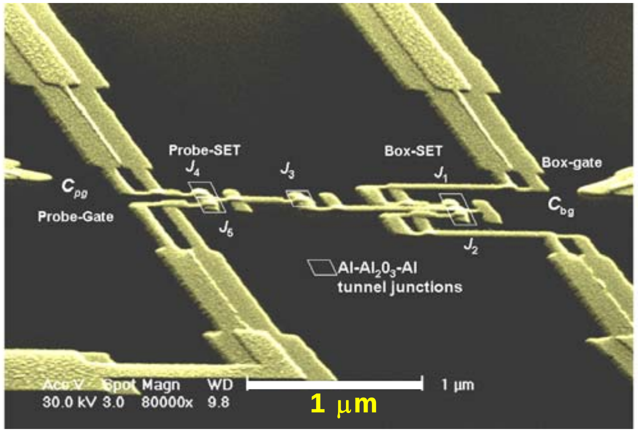

Suspending wire devices

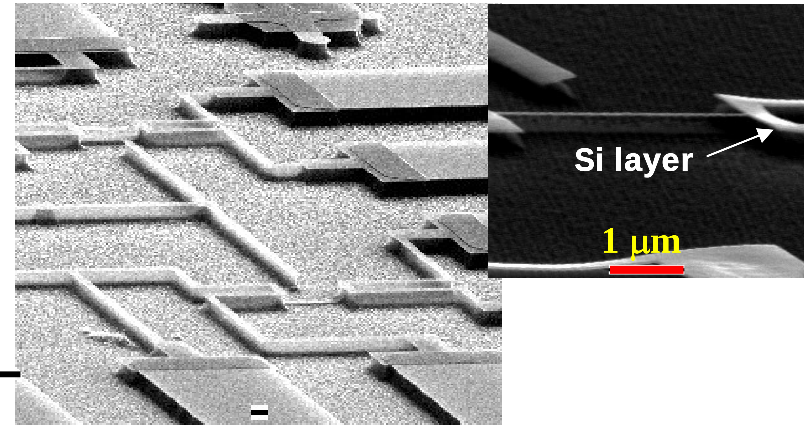

silicon nanoelectronics

7 nm Si-nanowire

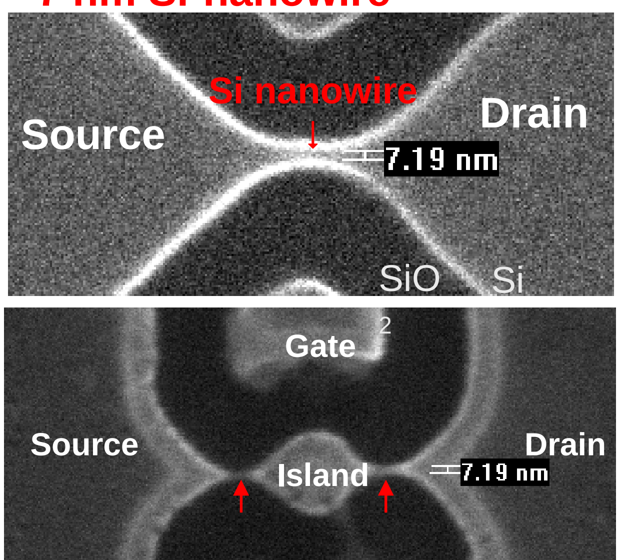

100nm Si-nanowire charge sensor

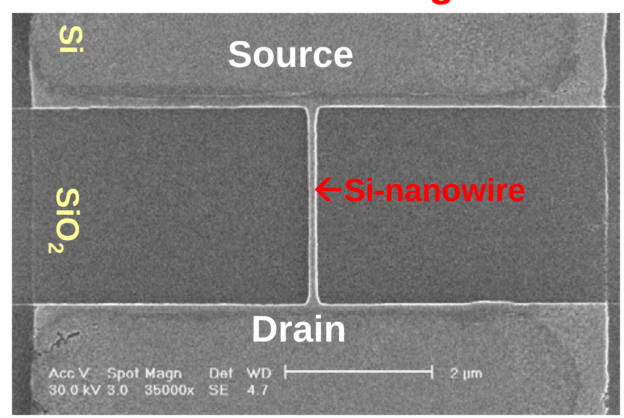

(Silicon On Insulator)

Molecular electronics

suspending nanoparticle devices

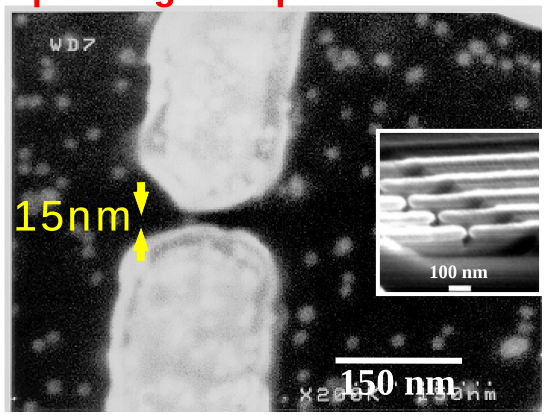

electrodes with a 5nm gap

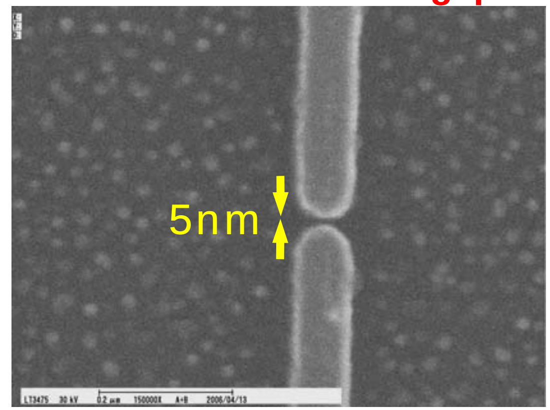

Nanopore-based molecular electronics

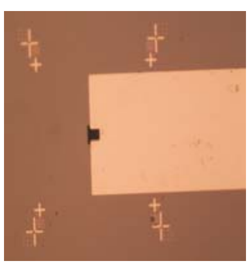

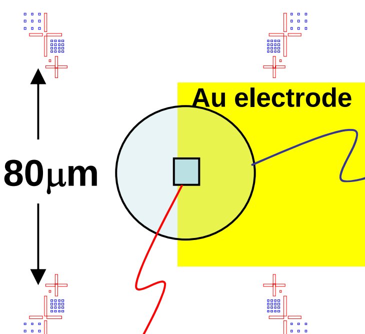

top electrode
+ molecules

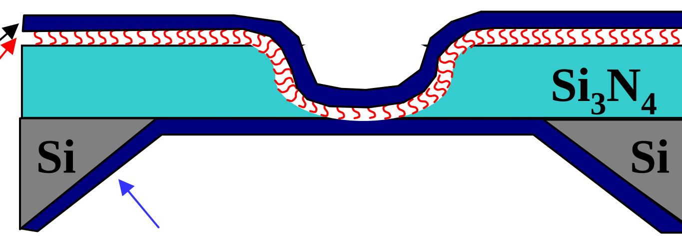

bottom electrode

Si_3N_4 membrane with a nanopore

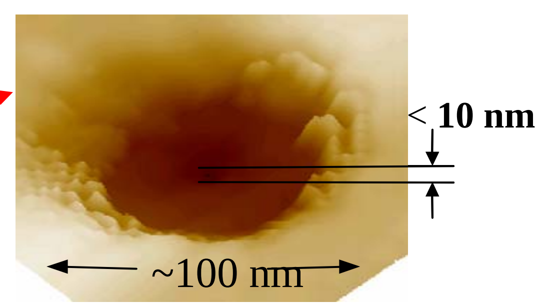

Nanowire electronic devices

Suspended
single wall carbon nanotube

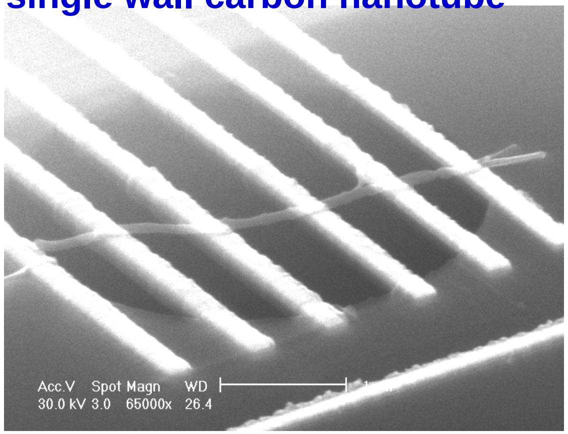

Bi_2Te_3 wire, 中研院物理所 陳洋元教授

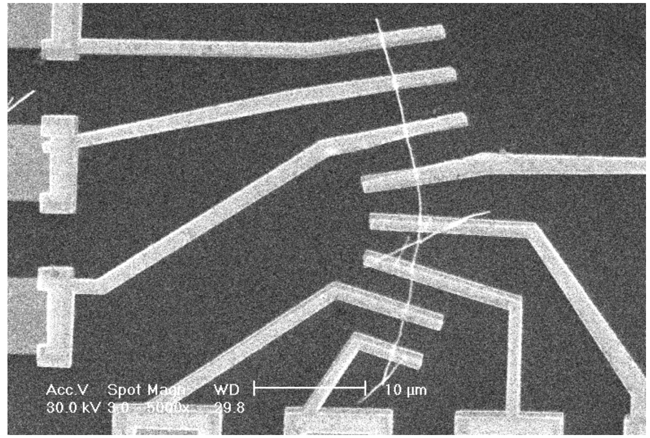

InN wire 台大凝態中心林麗瓊教授

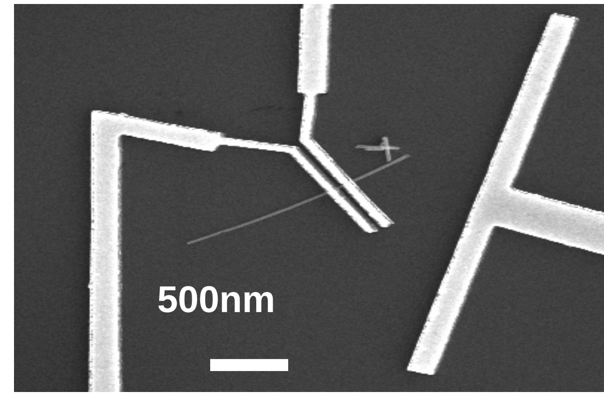

Multiwall carbon nanotube

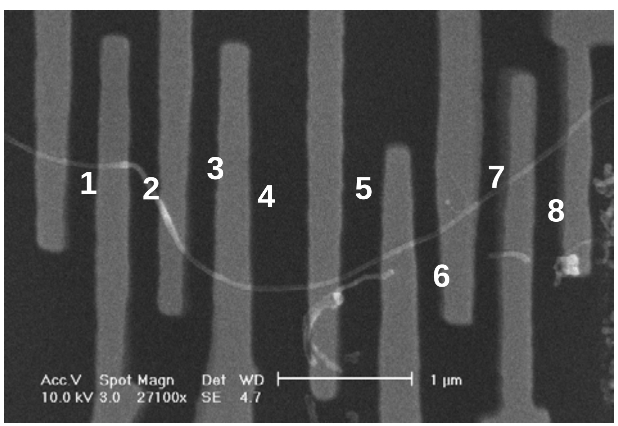

Ni_3Si_2 wire, 清大材料 陳力俊教授

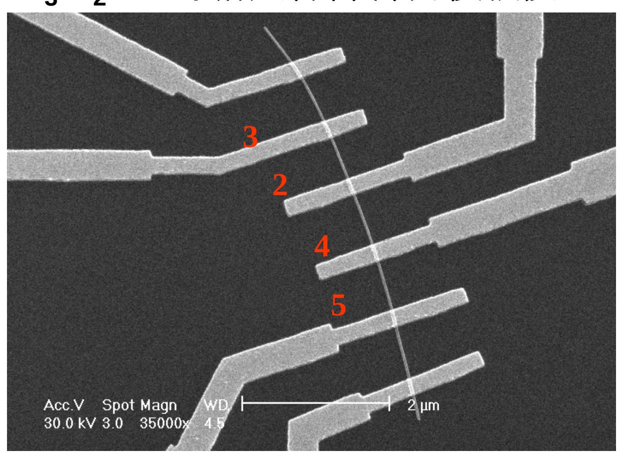

Carbon Helix 原分所陳益聰教授

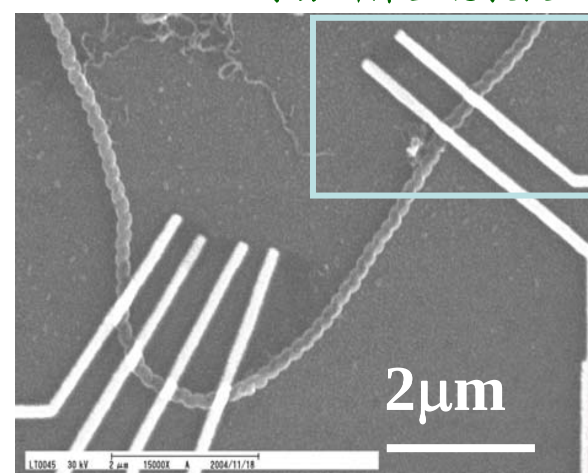

Photonic Crystals

Si-based 2D photonic crystal

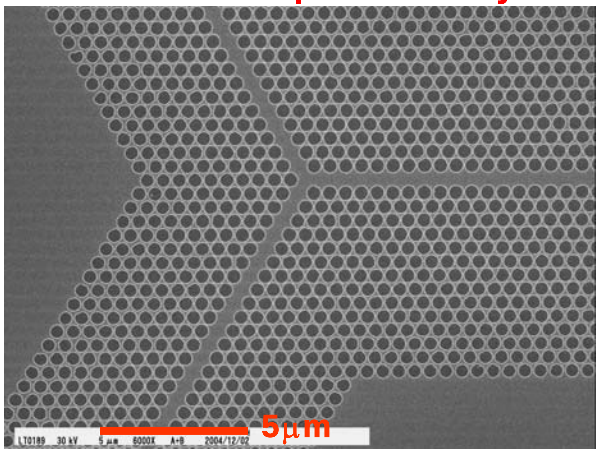

PMMA quasi-2D photonic crystal

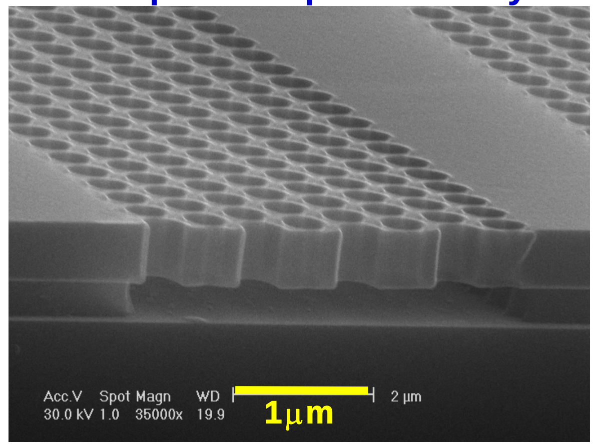

PMMA-LOR lattice structure

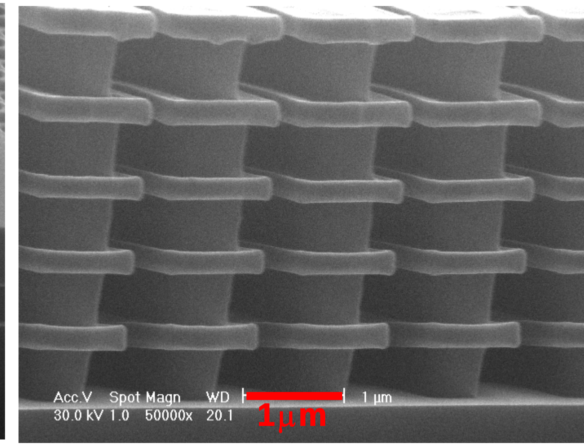

Hybrid nano-patterning technology

Au-nanoparticle pattern

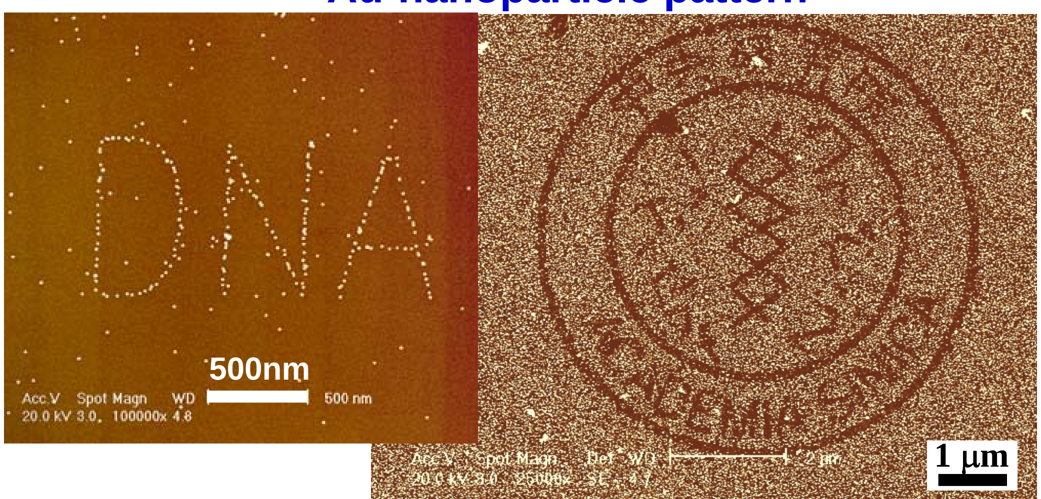

CdSe 2D-pillars

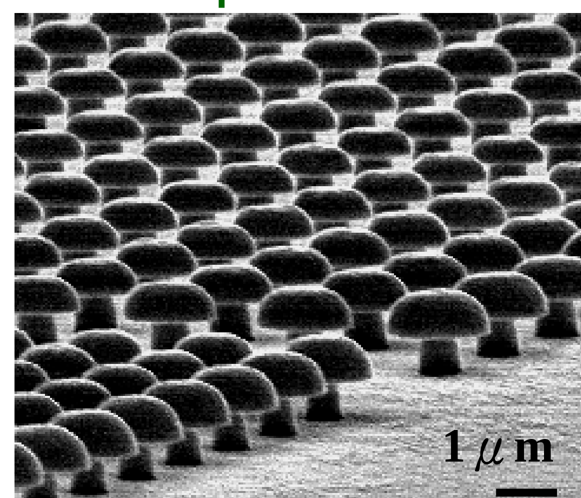

measurement setup

Available: 40mK, 5T

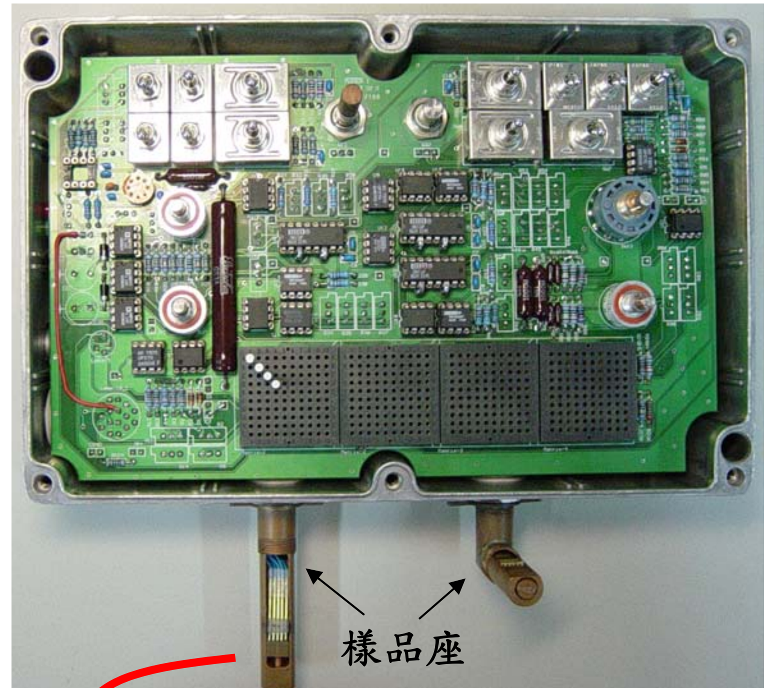

Characteristic length scales

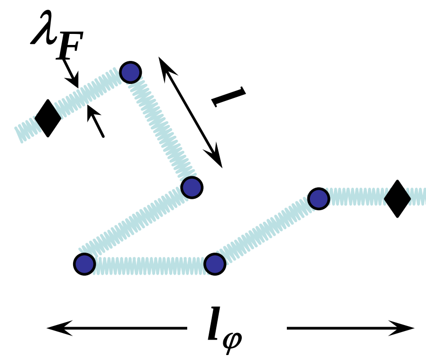

l : elastic mean free path

L_φ : phase-breaking length

Ballistic

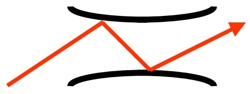

$(w, L) < l$

Mesoscopic

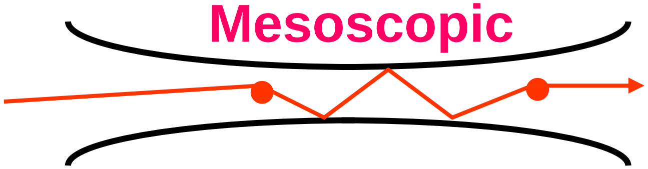

$l < (w, L) < L_\varphi$

Diffusive

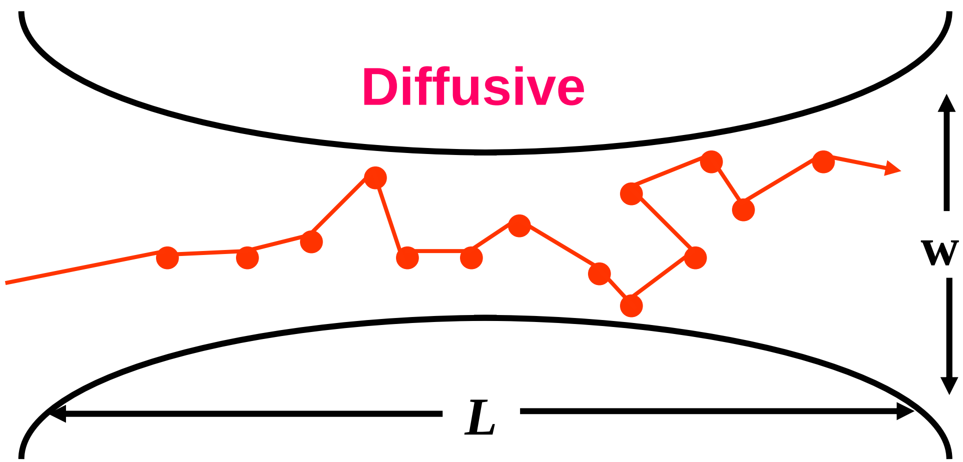

$L_\varphi << (w, L)$

Ballistic transport:
Length independent conductance

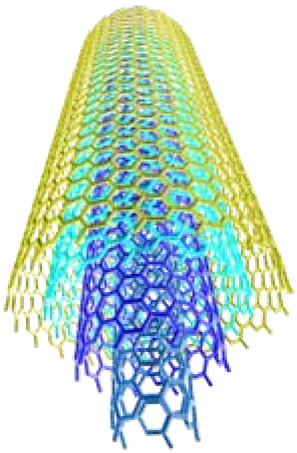

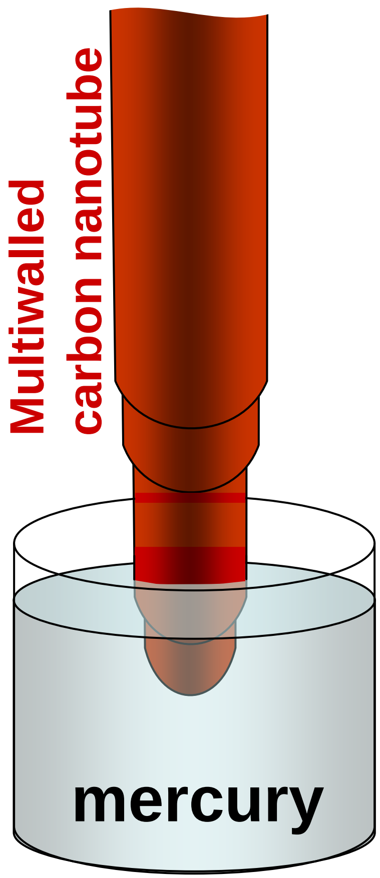

Walt de Heer,
Georgia Institute of Technology

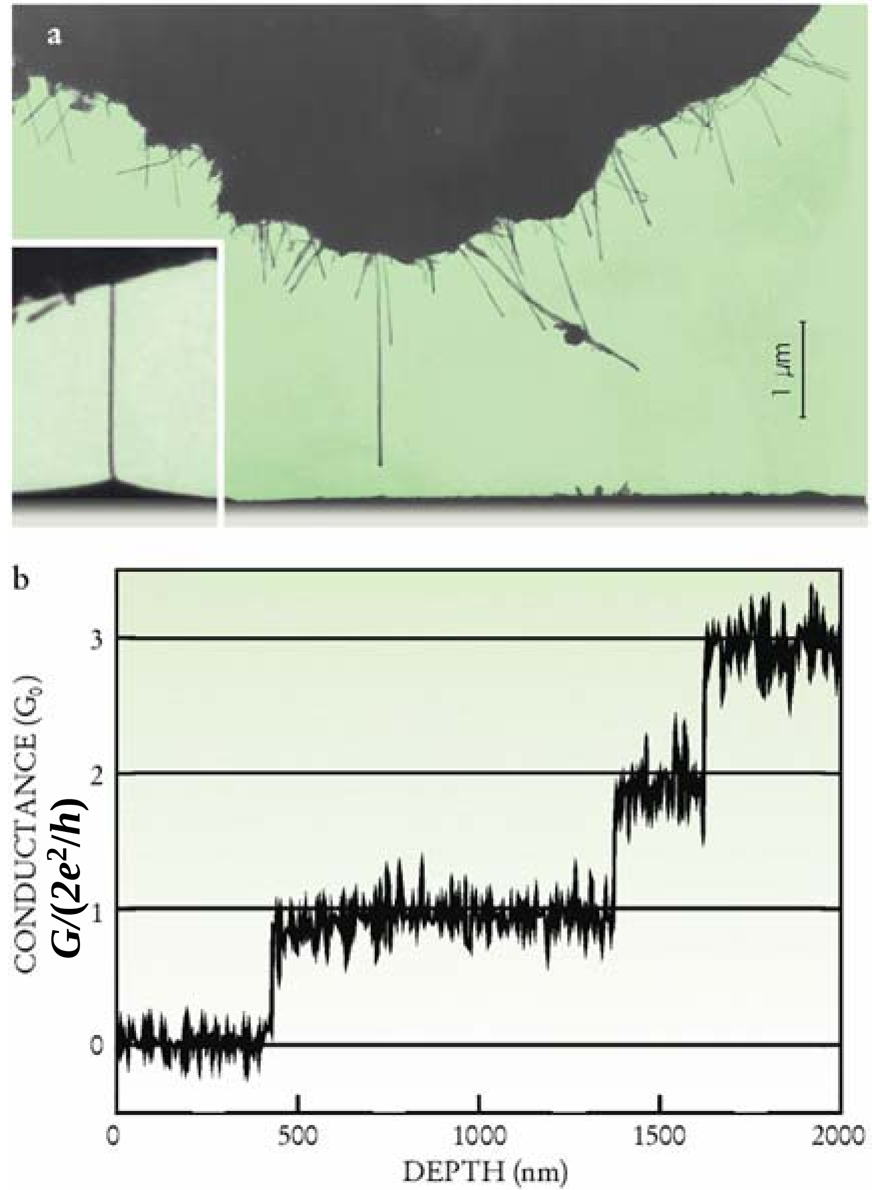

Ballistic system:

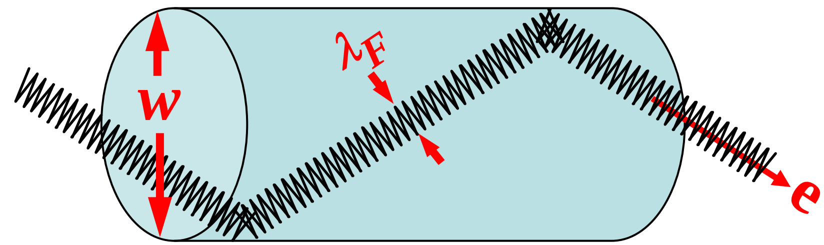

Devices with

1. Small diameter → only a few conduction channels

$$N \approx \pi w^2/\pi\lambda_F{}^2$$

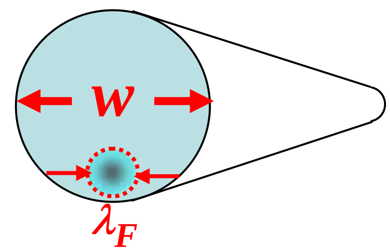

2. Small electron density → no *e*-*e* scattering
3. No impurity, no defect → no impurity scattering

$$G_0 = N\,2e^2/h$$

$$R_0 = \frac{1}{N}\frac{h}{2e^2} = \frac{R_Q}{N} \approx \frac{6.5k\Omega}{N}$$

R_Q: quantum resistance

Resistance independent of the length,
only determined by number of channels *N*

Resistance takes place at the macroscopic contacts

Two Dimensional Electron Gas (2DEG)

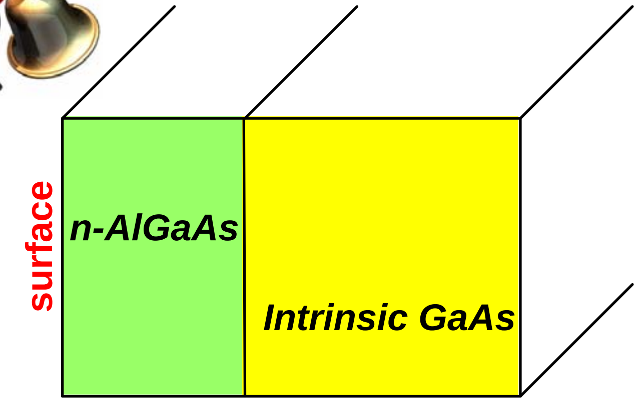

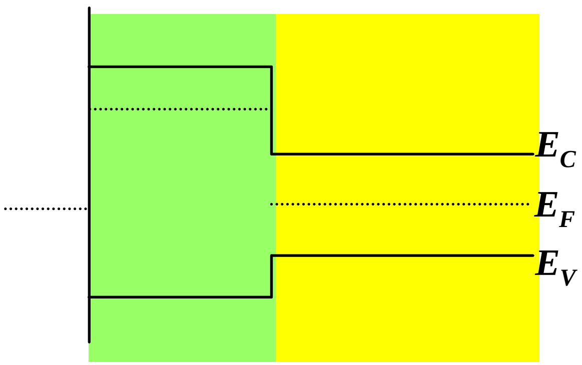

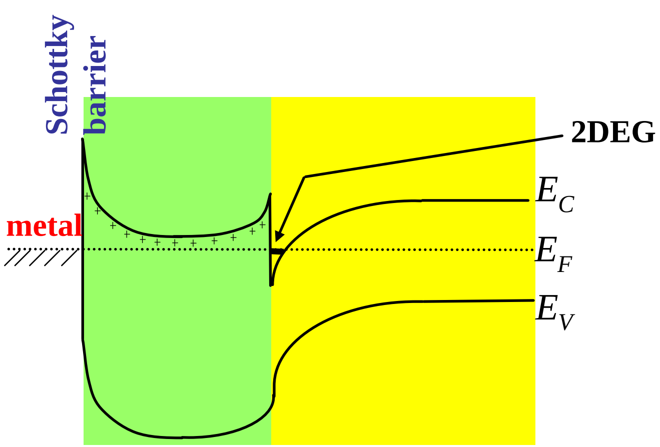

Formation:

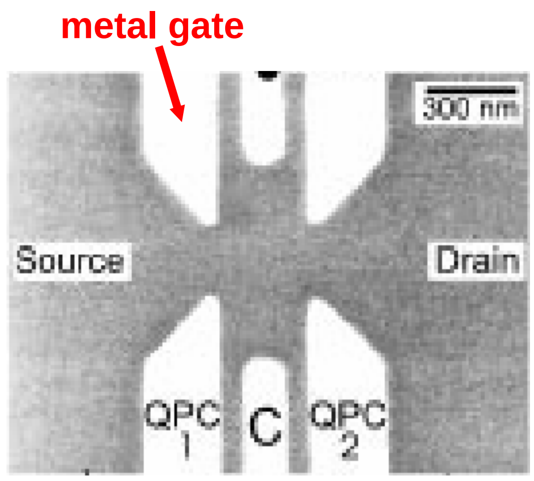

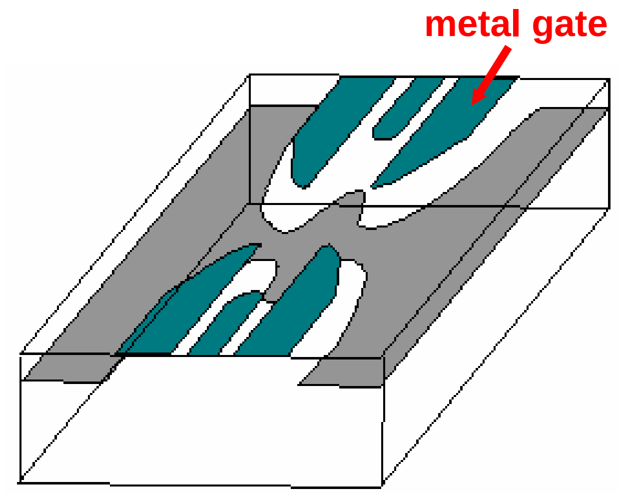

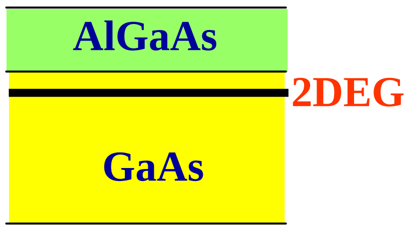

MOS type of 2DEG

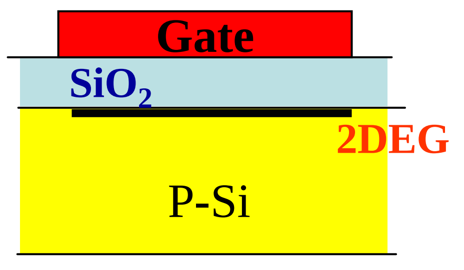

Conductance Quantization

Experiments on Quantum Point Contacts

B.J.van Wees et al. PRL 60, 848 (1988)

GaAs-AlGaAs heterostructure : 2DEG

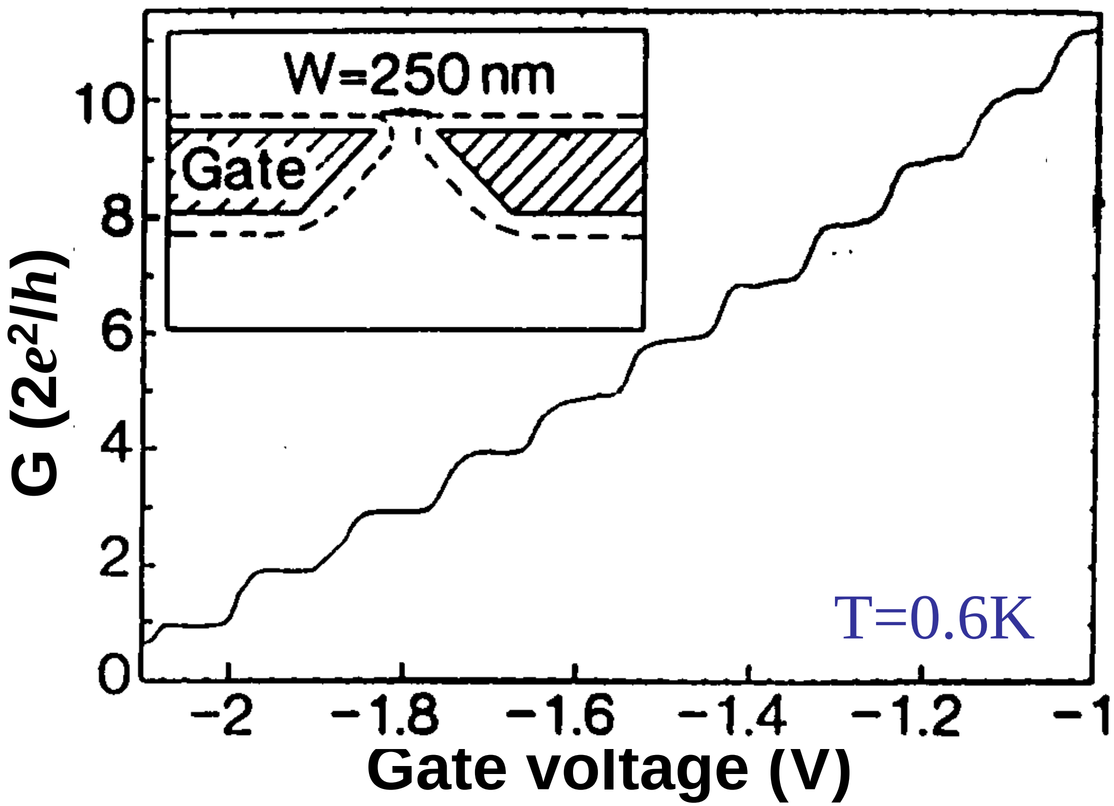

$$G = \frac{2e^2}{h} \sum_{n}^{N} T_n(E_F)$$

$$T_n(E_F) = \sum_{n=1}^{N} \left| t_{m\to n} \right|^2$$

For adiabatic constriction

$$t_{m\to n} = \delta_{nm}$$

For abrupt constriction

$$t_{m\to n} \neq 1$$

Optimized gate length

$$L_{opt} \approx 0.4\sqrt{\omega \lambda_F}$$

The origin of the conductance quantization

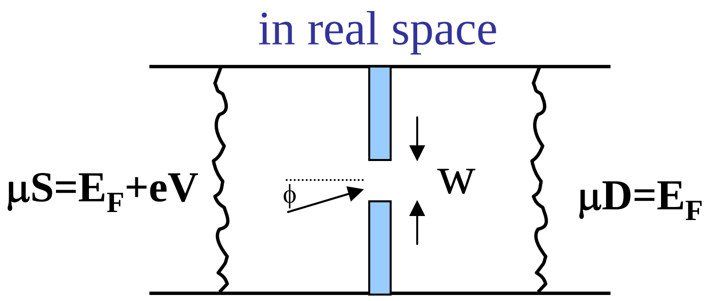

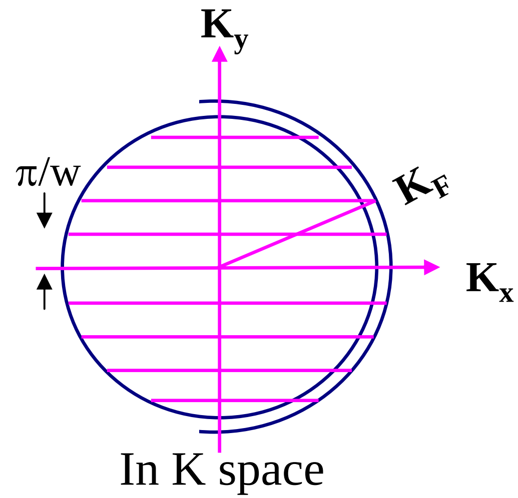

Diffusion current

transmission probability

$$I = e\sum_{n}^{N}\int_{E_F}^{E_F+eV} dE\,\rho_n(E)\,v_n(E)\,T_n(E) = \frac{2e}{h}eV\sum^{N}T_n(E_F)$$

1D Density of state

$$= \frac{1}{\pi}\left(\frac{dE_n}{dk}\right)^{-1}\frac{1}{\cos\phi}$$

Group velocity

$$= \frac{1}{\hbar}\left(\frac{dE_n}{dk}\right)\cos\phi$$

$$N = \frac{w}{\lambda_F/2}$$

Landauer Formula for contact conductance

$$G = \frac{2e^2}{h}\sum_{n}^{N}T_n(E_F) = \frac{2e^2}{h}\frac{W}{\lambda_F/2}$$

Origin of resistance

electron transport in disorder systems

impurities / defects / dislocation /other carriers

impurity potential

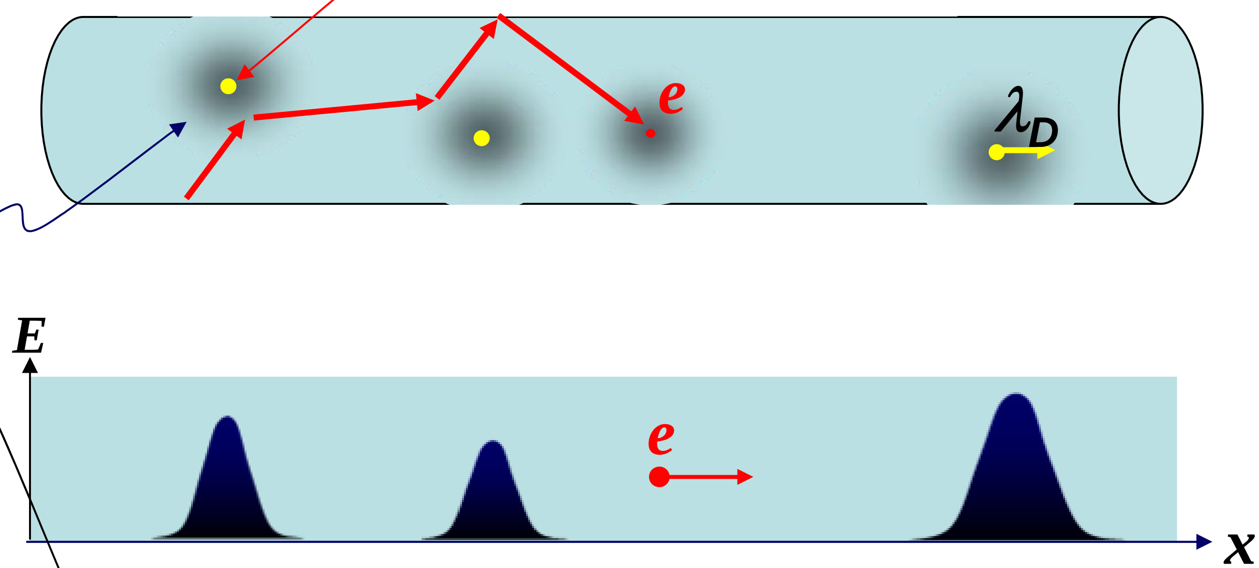

$$i\hbar \frac{\partial \Psi}{\partial t} = \left(-\frac{\hbar^2}{2m} \frac{\partial^2}{\partial x^2} + V \right) \Psi$$

Debye length $\lambda_D = \sqrt{\varepsilon k_B T / e^2 N_i}$

ε = dielectric permittivity,
k_B = Bolzmann constant,
T = absolute temperature,
e = electron charge

Quantum correction to the conduction

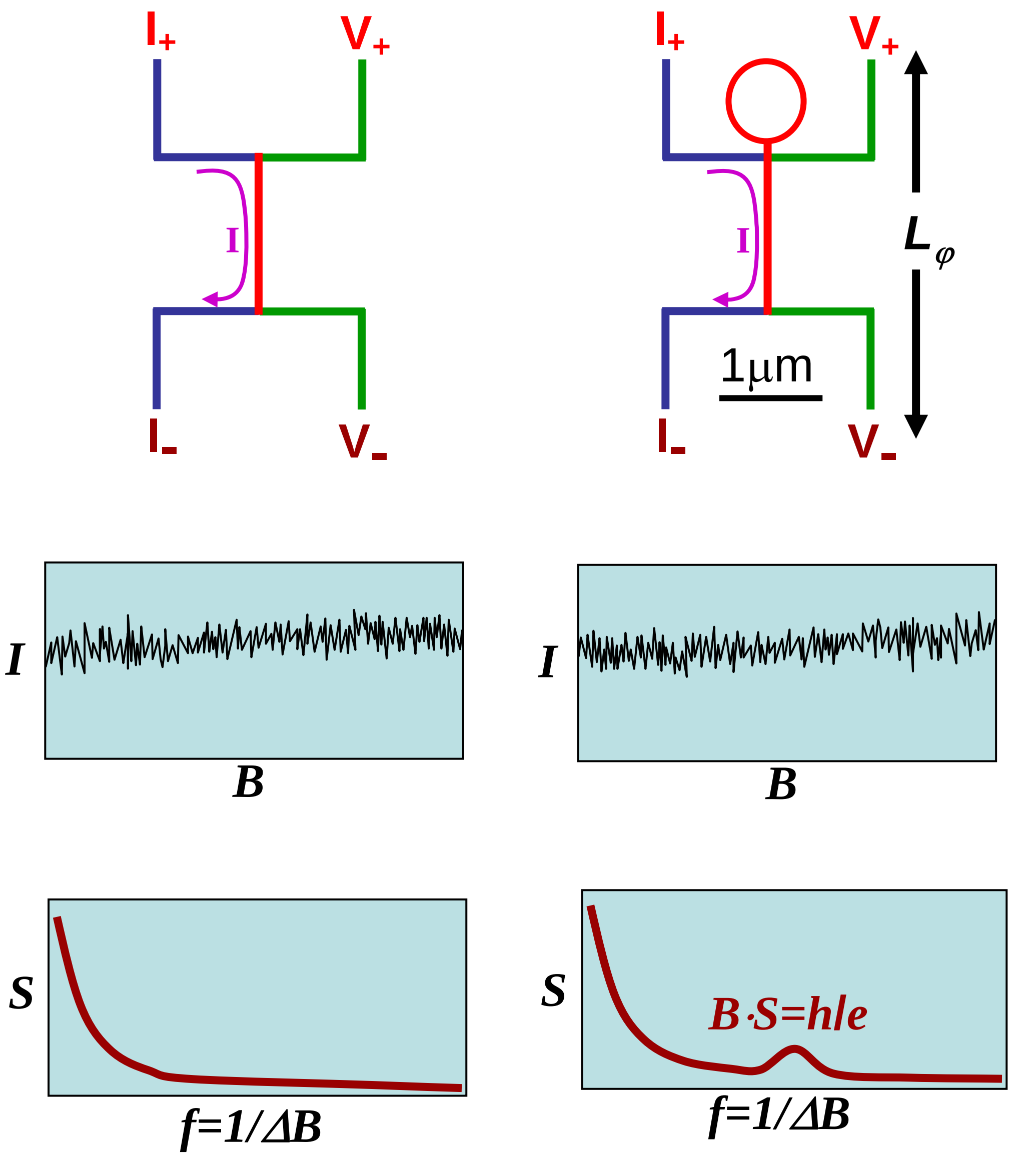

The quantum correction to the conductance can be strongly influenced by phase coherent regions extending beyond the probes and outside the classical current paths

Observation of h/e Aharonov-Bohm Oscillations in Normal-Metal Rings

R. A. Webb, S. Washburn, C. P. Umbach, and R. B. Laibowitz
IBM Thomas J. Watson Research Center, Yorktown Heights, New York 10598
(Received 27 March 1985)

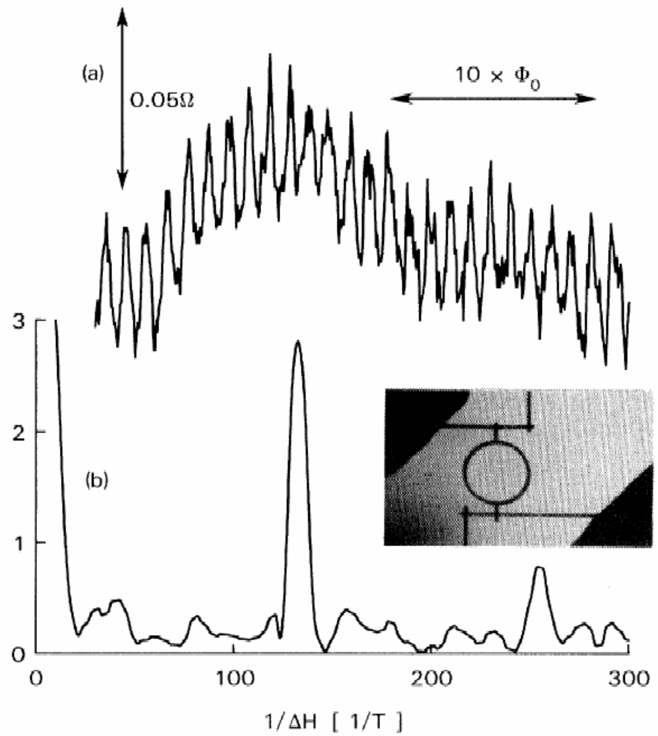

FIG. 1. (a) Magnetoresistance of the ring measured at $T=0.01$ K. (b) Fourier power spectrum in arbitrary units containing peaks at h/e and $h/2e$. The inset is a photograph of the larger ring. The inside diameter of the loop is 784 nm, and the width of the wires is 41 nm.

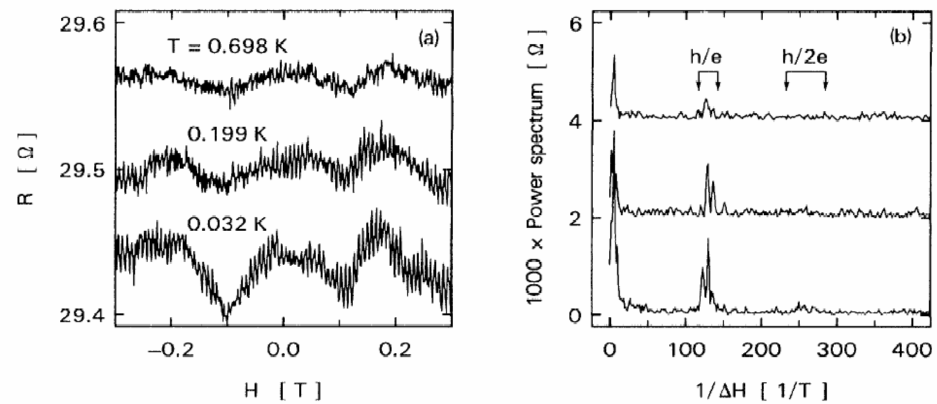

FIG. 2. (a) Magnetoresistance data from the ring in Fig. 1 at several temperatures. (b) The Fourier transform of the data in (a). The data at 0.199 and 0.698 K have been offset for clarity of display. The markers at the top of the figure indicate the bounds for the flux periods h/e and $h/2e$ based on the measured inside and outside diameters of the loop.

Aharonov-Bohm effect

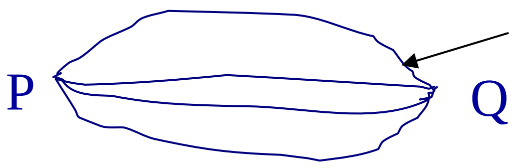

Probability for P → Q

$$W_{P\to Q} = \left|\sum_i A_i\right|^2 = \underbrace{\sum_i |A_i|^2}_{\text{Clasical diffusion}} + \underbrace{\sum_{i\neq j} A_i A_j^*}_{\text{Quantum interference}}$$

electrons pick a phase φ when traveling along a path P

$$\varphi = \frac{e}{\hbar}\int_P A\cdot dx$$

phase difference between two paths with the same ends

$$\phi = \frac{1}{\hbar}\int_P^Q A\cdot dl_1 - \frac{1}{\hbar}\int_P^Q A\cdot dl_2 = \frac{1}{\hbar}\int_P^Q A\cdot dl_1 + \frac{1}{\hbar}\int_Q^P A\cdot dl_2 = \frac{1}{\hbar}\oint A\cdot dl$$

$$= \frac{2e}{\hbar}\int (\nabla\times A)\cdot dS = \frac{2e}{\hbar}\int BdS = 2\pi\frac{B\cdot S}{h/2e}$$

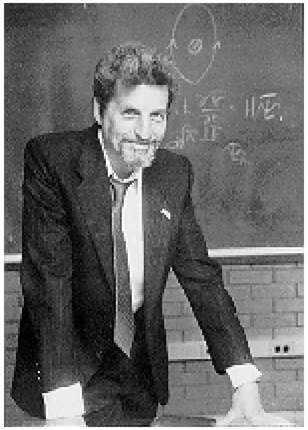

Yakir Aharonov

Probability for back-scattering

$$W_{P\leftrightarrow P} = 2|A|^2 + 2|A|^2\cos\left(2\pi\frac{B\cdot A}{h/2e}\right) \rightarrow \text{period} = h/2e$$

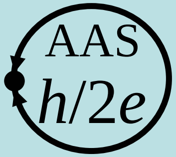

Aharonov-Casher effect

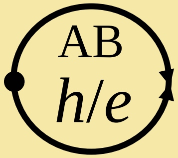

Aharonov-Bohm effect

Weak localization

takes place for length scale < L_ϕ

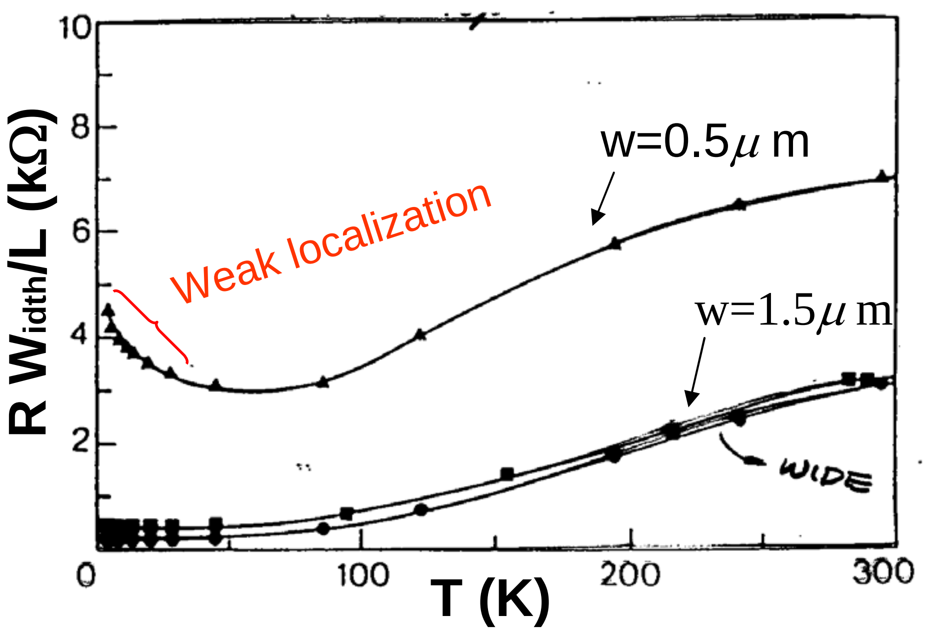

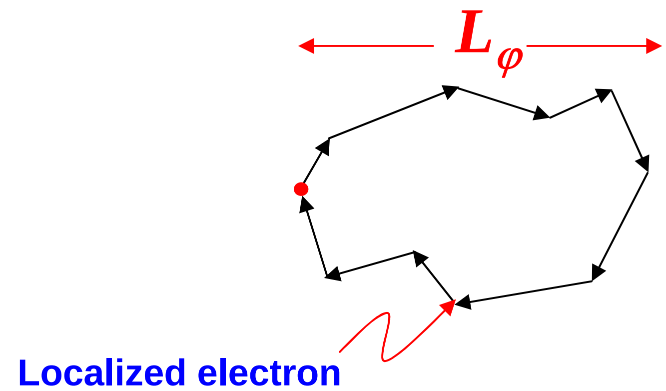

Other possible explanations:
- **electron-electron interaction**
- **Kondo-effect**

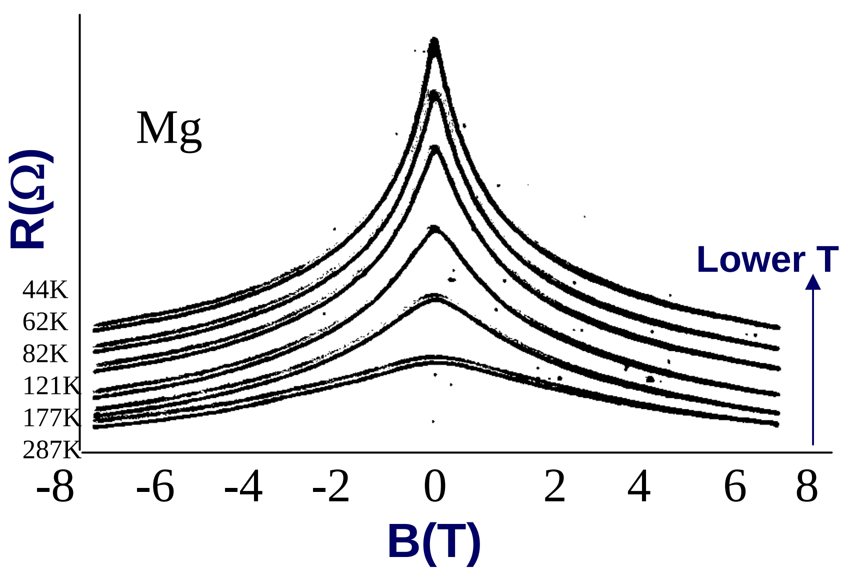

time reversal symmetry

Magnetic field:
break the
time reversal symmetry

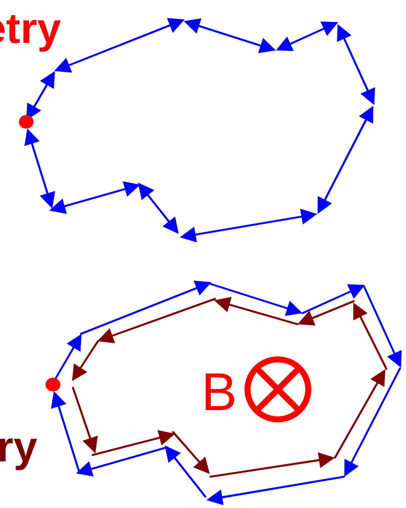

Hopping conduction in disordered systems

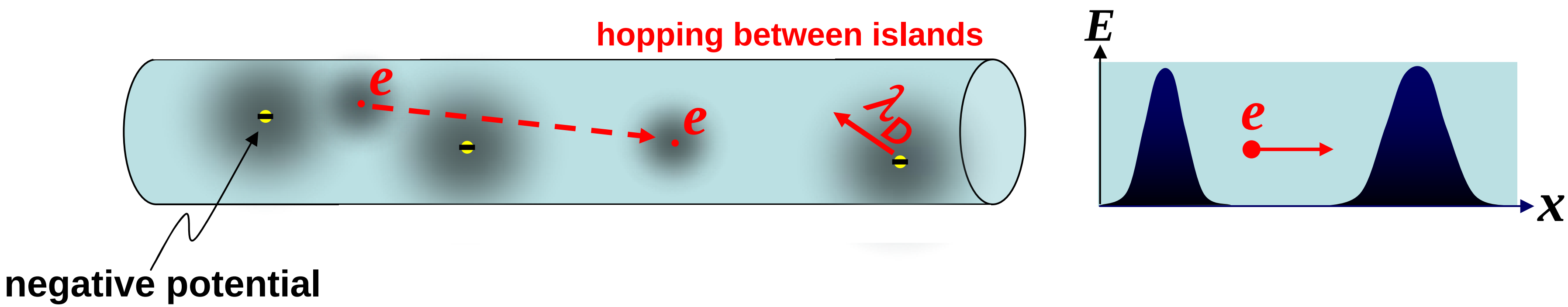

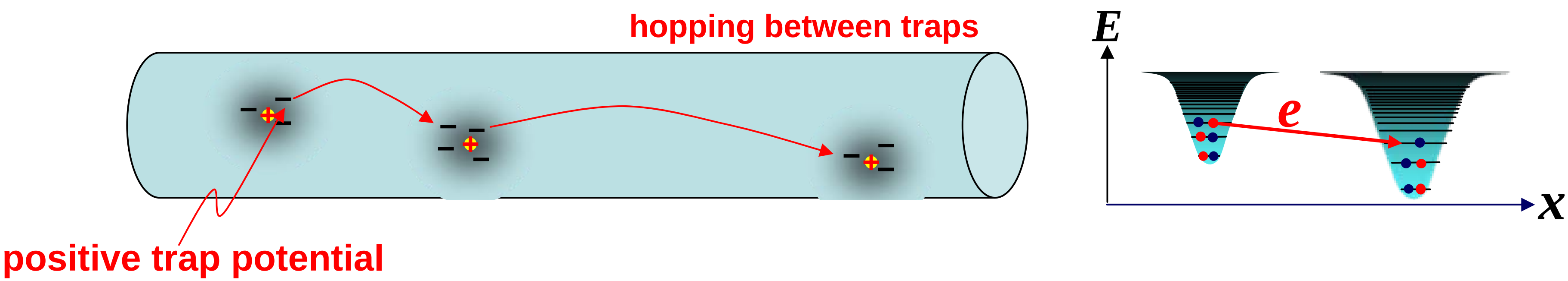

Metallic grains

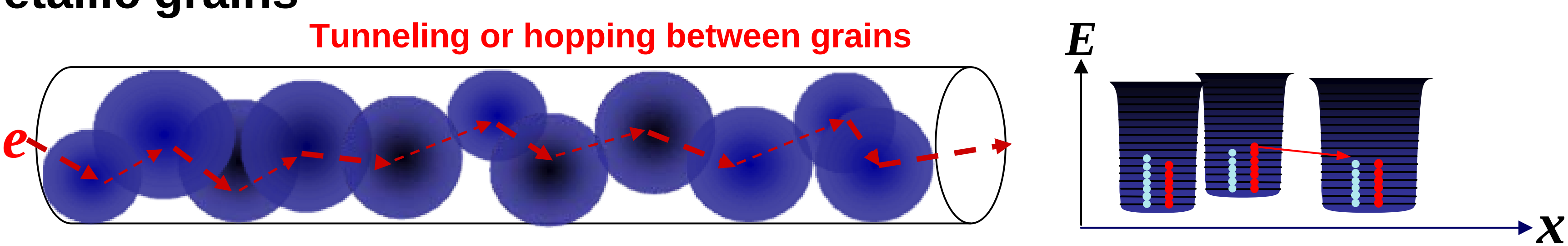

Hopping transport

R_o increases with decreasing temperature

Nearest neighbor hopping (Arrhenius form)

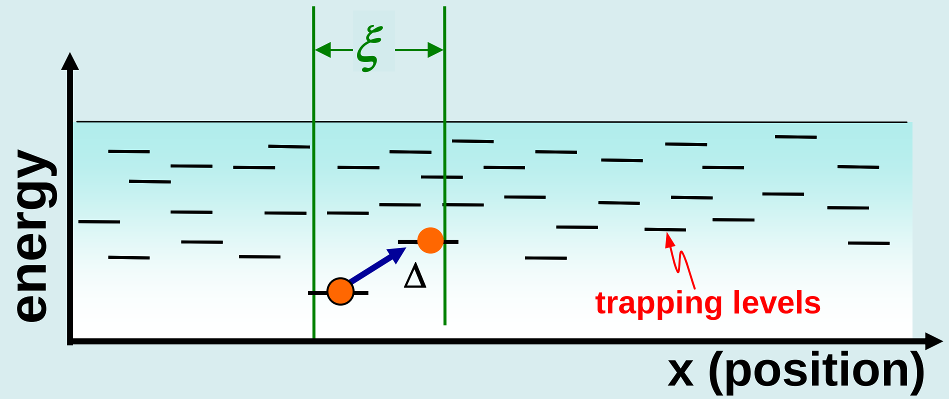

$$R_0 = R_A \exp\left(\frac{\Delta}{k_B T}\right)$$

Presence of a **hopping barrier**; thermally activated hopping (such as Coulomb blockade)

Mott Variable range hopping

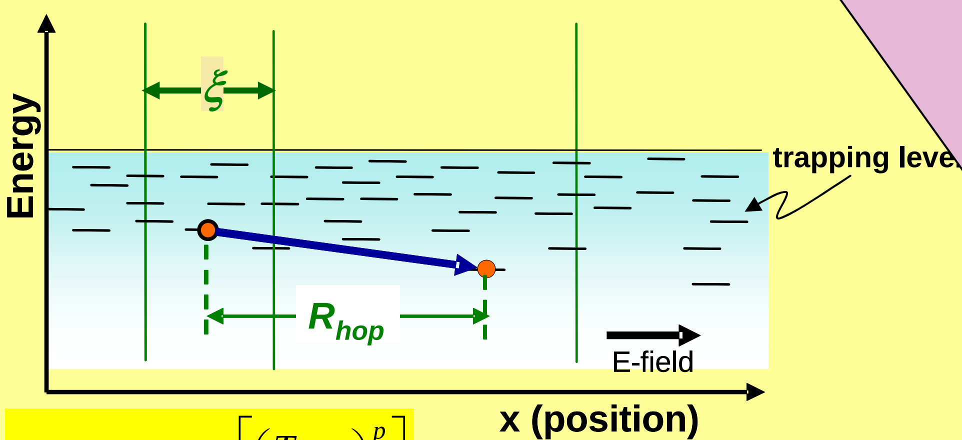

$$R_0 = R_A T^S \exp\left[\left(\frac{T_{Mott}}{T}\right)^p\right]$$

T_{Mott} = Mott characteristic temperature

$$p = \frac{1}{1+d}$$ d = system dimensionality

Efors-Shklovskii Variable range hopping

when Coulomb interaction is considered

$$R_0 = R_A T^S \exp\left[\left(\frac{T_{ES}}{T}\right)^{1/2}\right]$$

power-law dependence in DOS near E_F

$$N(E) = N_0 |E - E_F|^{\gamma}$$

For 3D, γ=2

Nonlinear IV_b characteristics

Quantum origin of energy level broadening

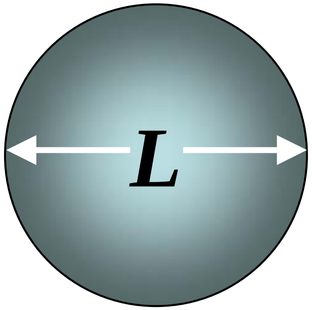

broadening of quantized levels

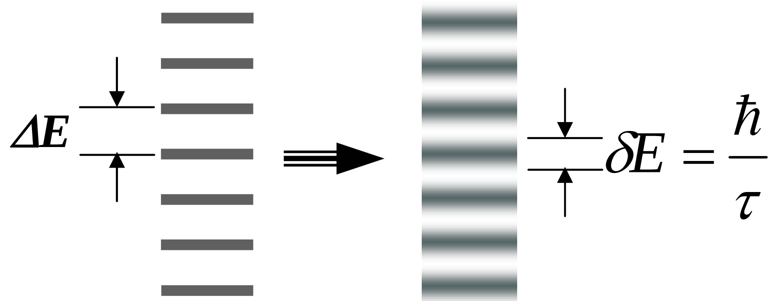

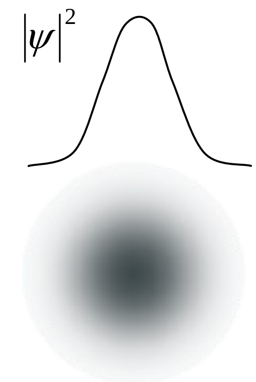

τ = time for electron to travel through the grain

in ballistic regime: $\tau = L/v_F$

---

in diffusive regime: $\tau = L^2/D$

Einstein relation: $\sigma = e^2 D N_0(E_F) \Rightarrow \delta E \approx (\sigma h/e^2)\left[L^2 N_0(E_F)\right]^{-1}$

Level spacing : $\Delta E = [L^d N_0(E_F)]^{-1}$

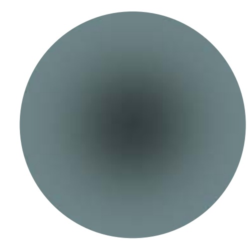

Thouless ratio $g \equiv \frac{\delta E}{\Delta E} \approx \frac{h}{e^2}\sigma L^{d-2} = \frac{G}{e^2/h}$

$g < 1$ (R>26kΩ) $\Rightarrow$ localized state

$g > 1$ (R<26kΩ) $\Rightarrow$ extended state

Inter-grain coupling induced level broadening

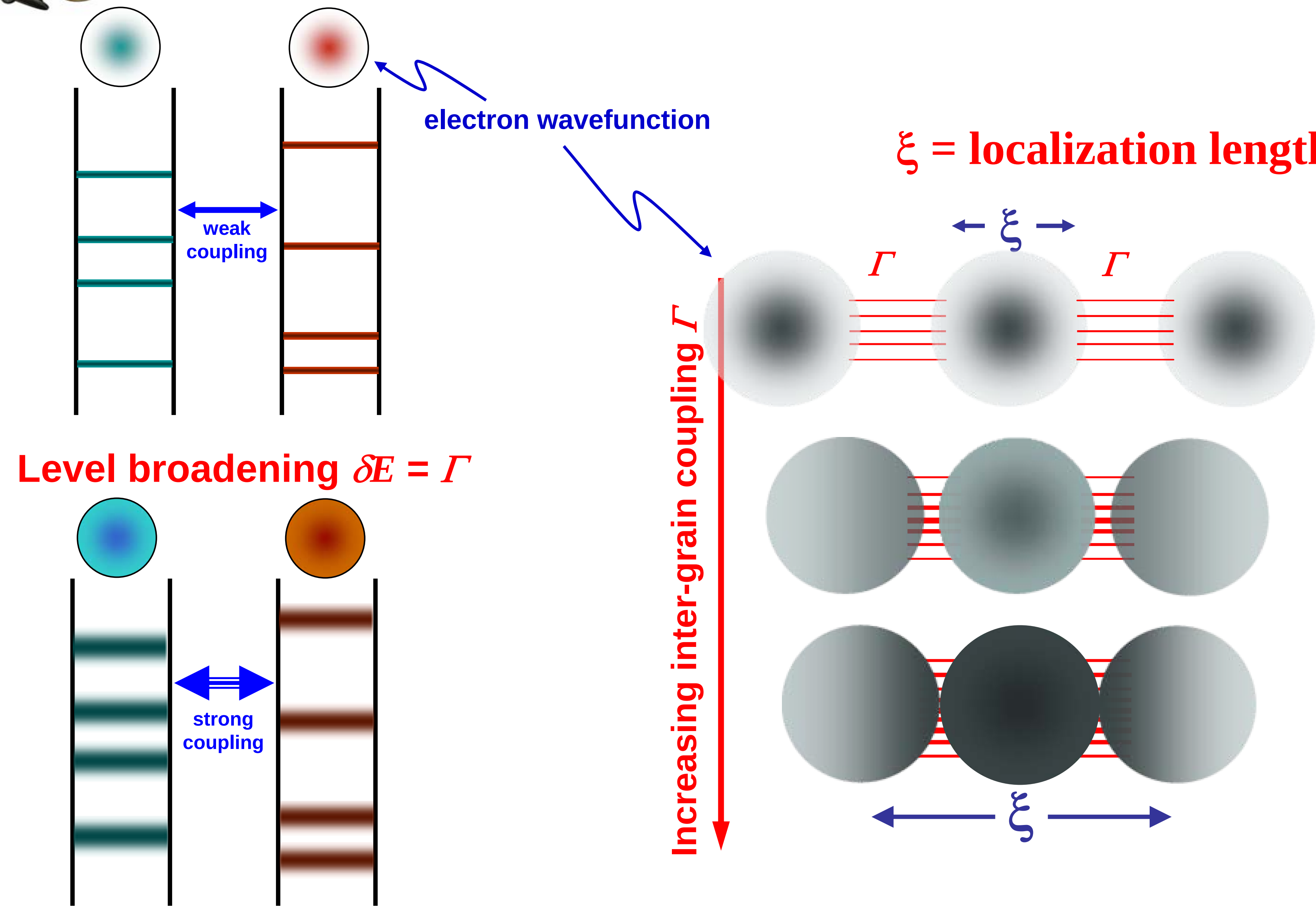

Resonate tunneling between coupled quantum dots

For very weak inter-coupling, two possible states exist : |R⟩ and |L⟩
With finite coupling Γ, |R⟩ and |L⟩ mix and form two eigenstates |A⟩ and |S⟩

Coupling strength = Γ
tunneling rate $\gamma = \Gamma / \hbar$
level broadening $\delta E = \Gamma$

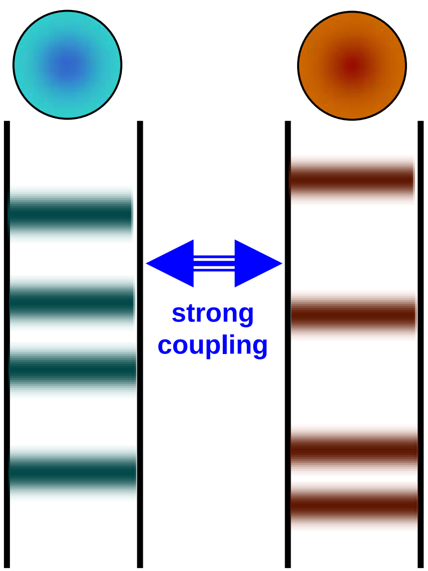

$$|S\rangle = \frac{1}{\sqrt{2}}\left(|R\rangle + |L\rangle\right)$$

Symmetric |S⟩ with eigenenergy E_S

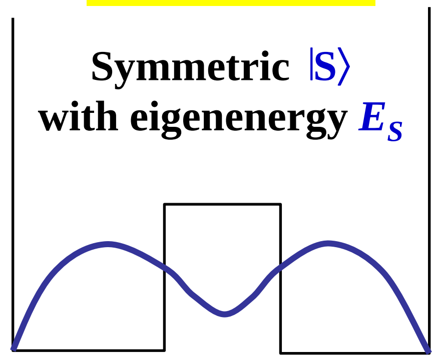

$$|A\rangle = \frac{1}{\sqrt{2}}\left(|R\rangle - |L\rangle\right)$$

Anti-symmetric |A⟩ with eigenenergy E_A

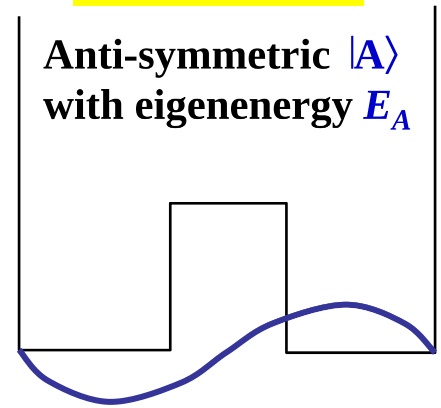

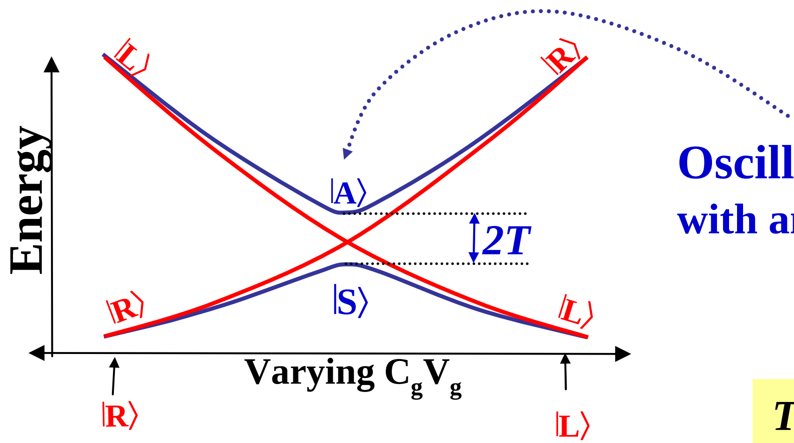

Oscillation between |R⟩ and |L⟩ with angular frequency

$$\omega = \frac{E_A - E_S}{\hbar} = \frac{2T}{\hbar}$$

T = coupling constant

Weakly coupled dots

Microwave spectroscopy of a quantum-dot molecule
T. H. Oosterkamp, T. Fujisawa, W. G. van der Wiel, K. Ishibashi, R. V. Hijman, S. Tarucha & L. P. Kouwenhoven (Nature, v. 395, p. 873, Oct. 1998)

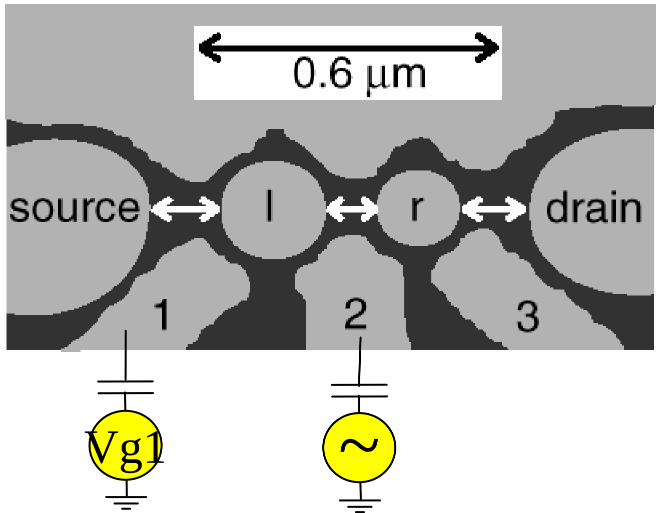

Photon assisted tunneling

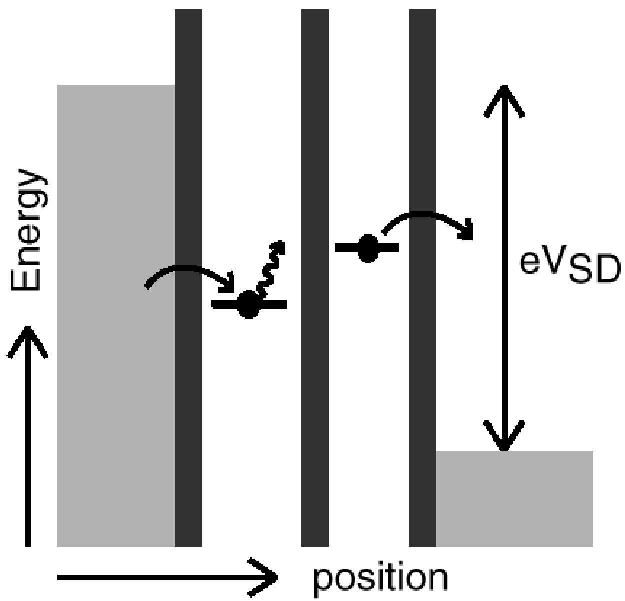

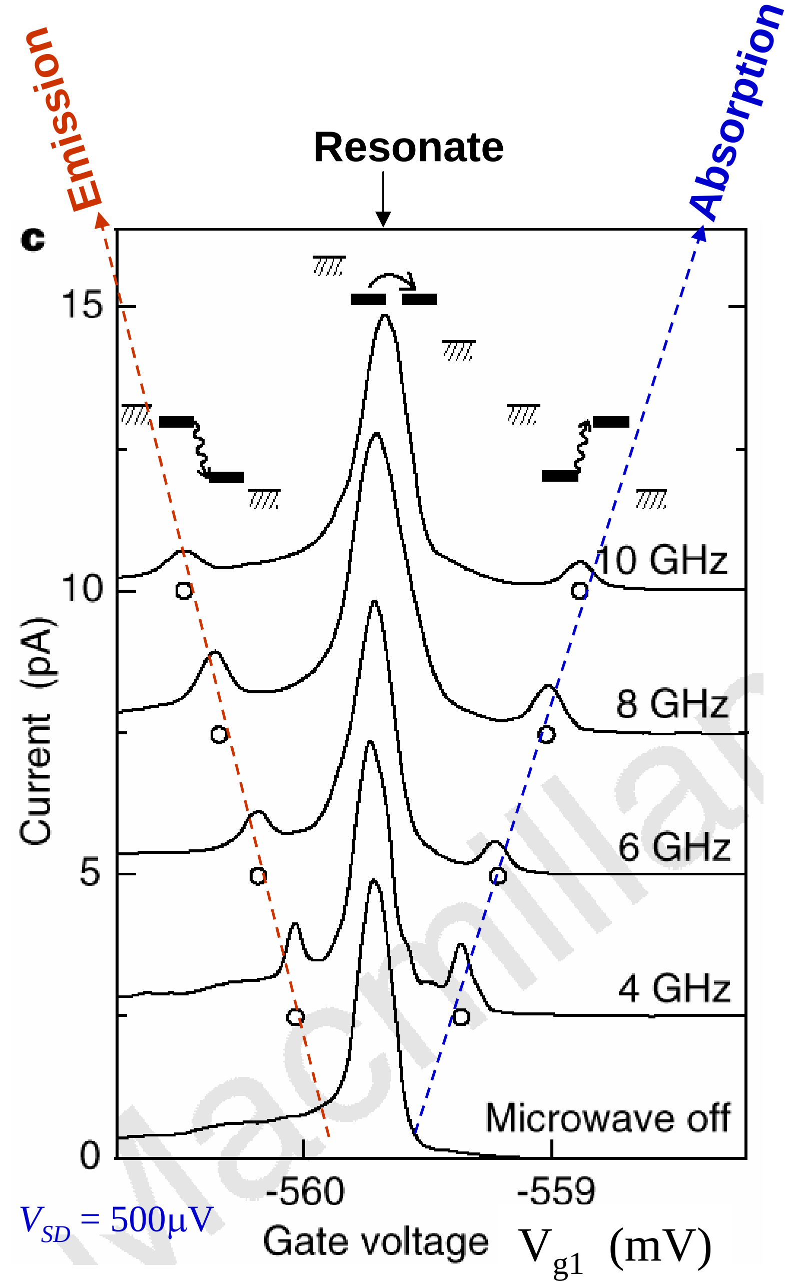

Strongly coupled dots

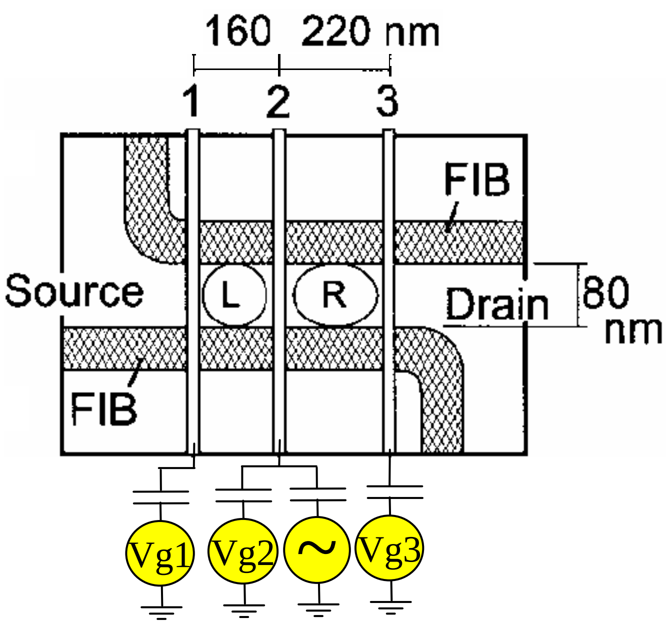

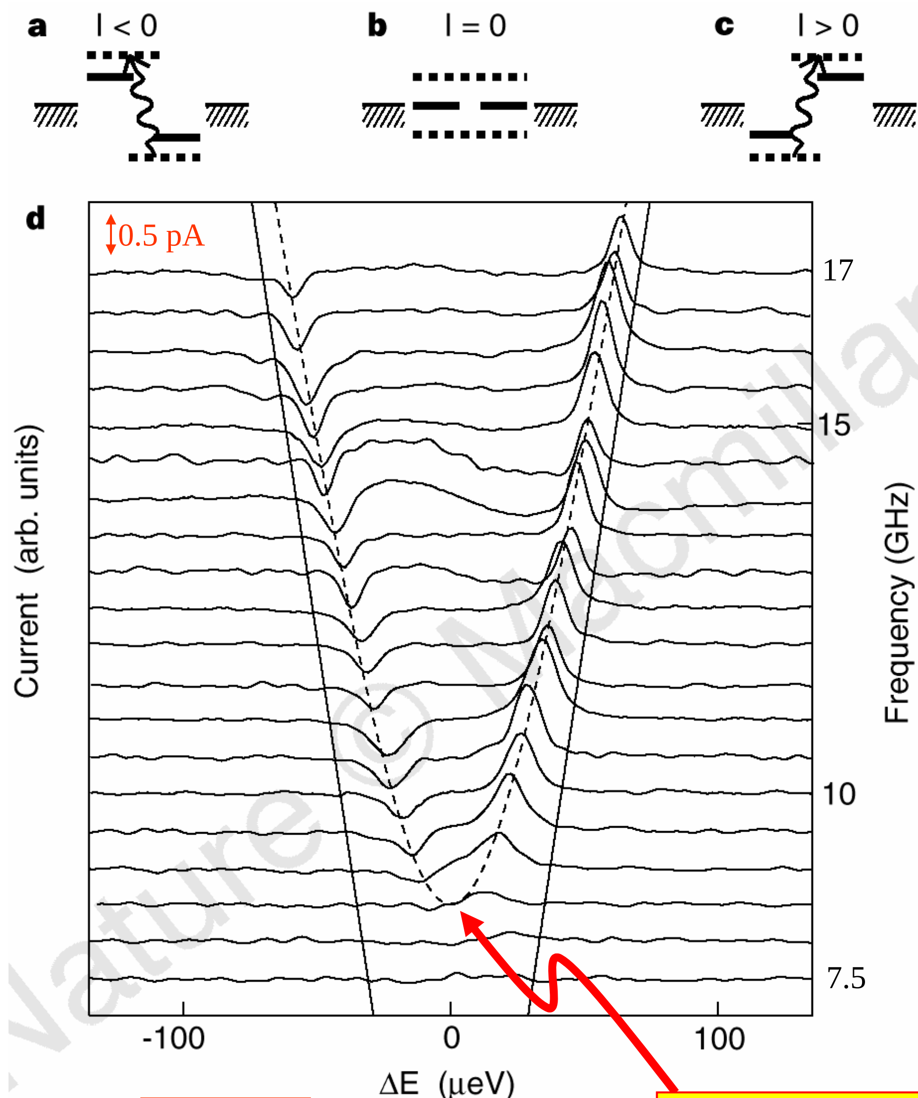

V_{SD}=0

$$hf = \sqrt{\Delta E^2 + (2\Gamma)^2}$$

The Quantum Bit

A two-level system (psudo-spin) ⟹ a quantum bit (qubit)

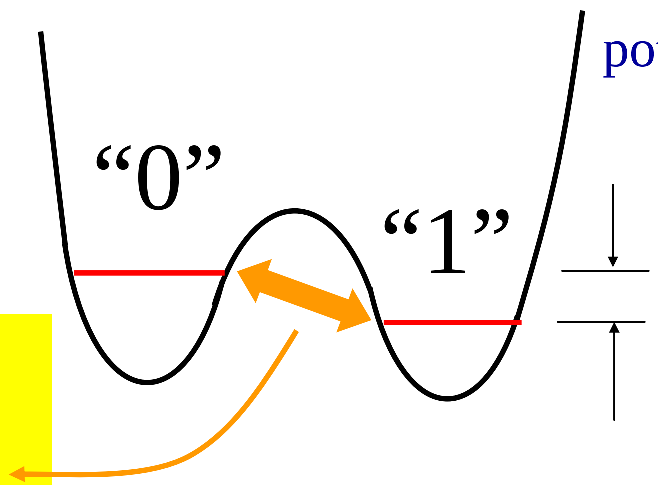

ε, the energy difference for $|\mathbf{0}\rangle$ and $|\mathbf{1}\rangle$

Δ, the coupling energy for $|\mathbf{0}\rangle$ and $|\mathbf{1}\rangle$

Provided by quantum tunneling ⟹ Level repulsion

Classical Boolean bits vs. Quantum bits (Qubits)

Classical	Quantum
0	$\lvert 0\rangle$
1	$\lvert 1\rangle$
No classical analogue	$(\lvert 0\rangle \pm \lvert 1\rangle)/\sqrt{2}$ **Superposition**
	$\Psi = \sum_{x=00...0}^{11...1} c_x \lvert x\rangle$ **Entanglement**
	e.g. $(\lvert 01\rangle \pm \lvert 10\rangle)/\sqrt{2}$

can perform calculations on all 2^n bits at once (quantum parallelism)

NOT operator

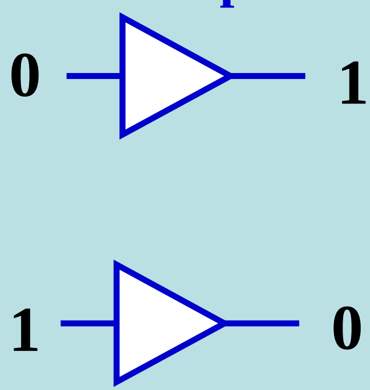

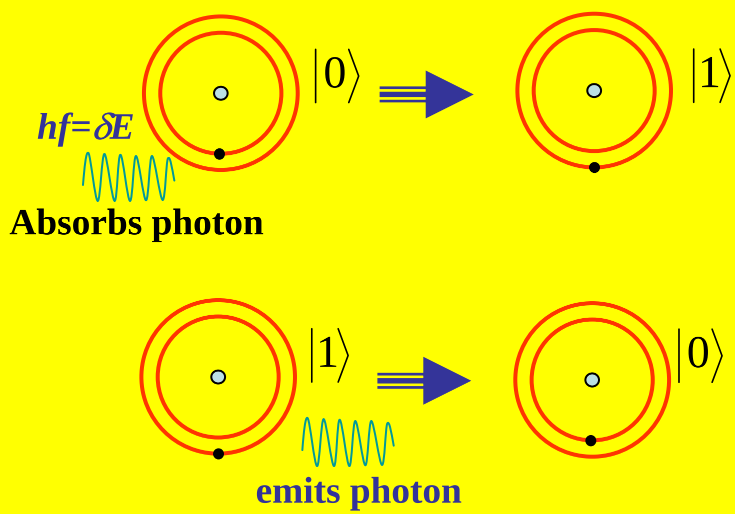

Can also flip bits only halfway

Superconducting Quantum Bits

Charge qubit: NEC, Saclay, Chalmers, Yale…

charge number

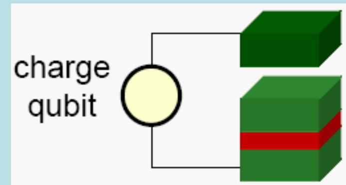

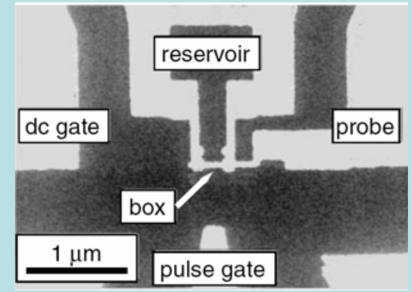

flux qubit: Delft, Stony Brook, Berkeley…

flux number

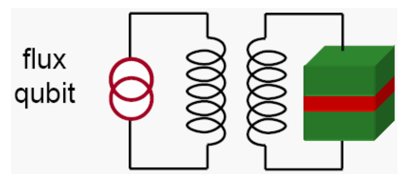

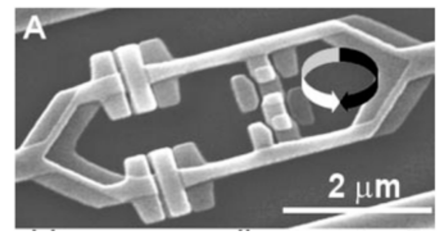

phase qubit: NIST, Kansas

phase difference across a junctio

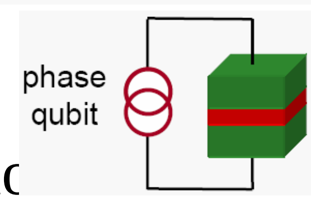

And other proposals, such as Andreev qubit

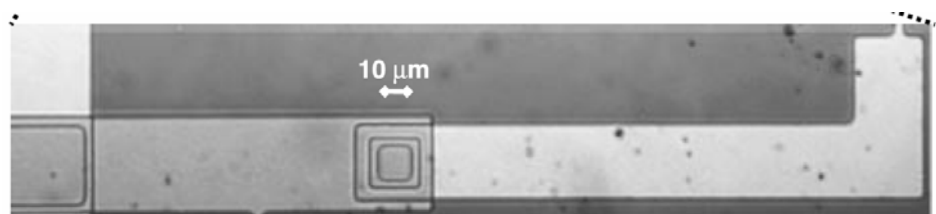

What is a superconductor?

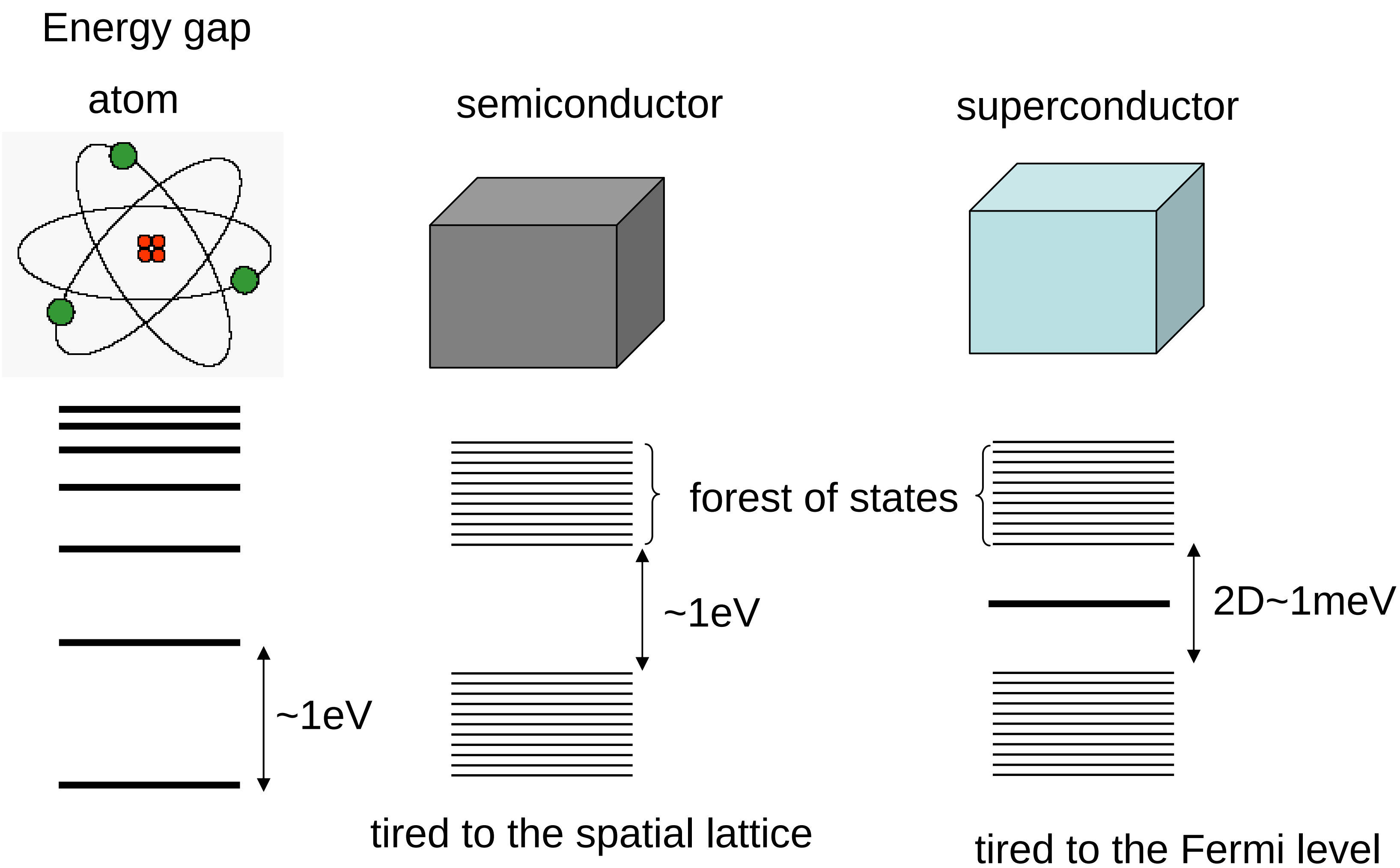

Cooper pairs are like bosons in a BEC,
except size of Cooper pair (electron separation) ~ ξ

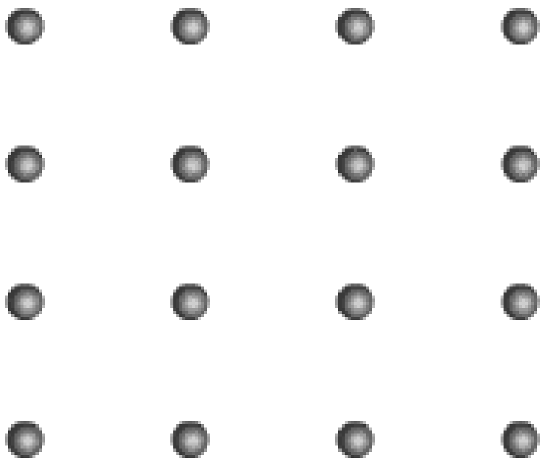

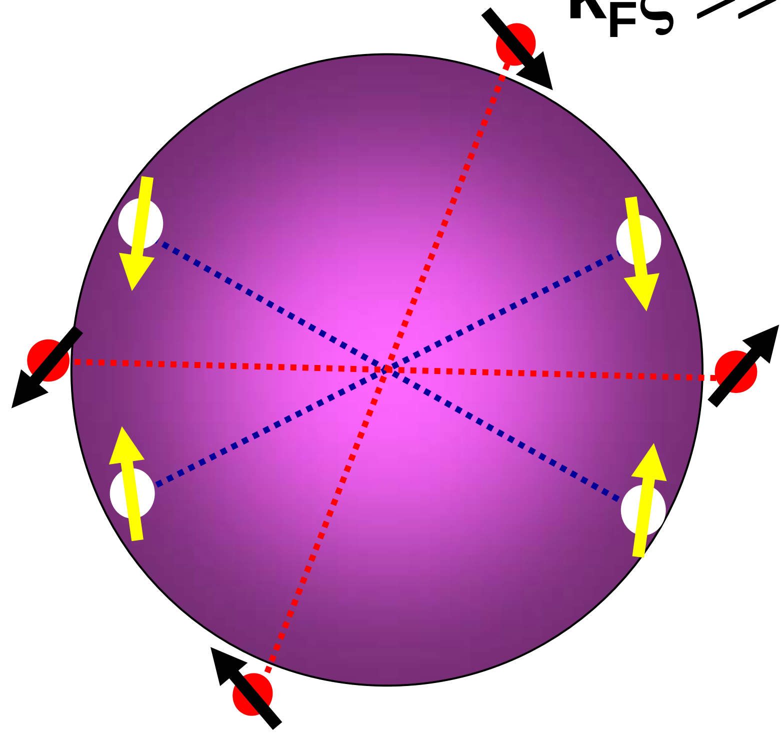

Fermi sphere for a superconductor

$$\psi(\vec{r}) \sim \left\langle c_{\vec{k}\uparrow} c_{-\vec{k}\uparrow} \right\rangle \sim \left|\psi\right| e^{i\varphi(\vec{r})}$$

Josephson junction

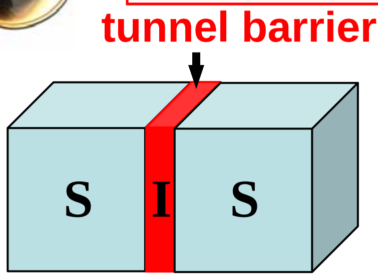

$$E_J = \frac{\Delta}{2}\frac{R_Q}{R_N}$$

Quantum resistance $R_Q \equiv \frac{h}{4e^2}$

Tight binding model: particles hopping in a 1D chain in Hilbert space

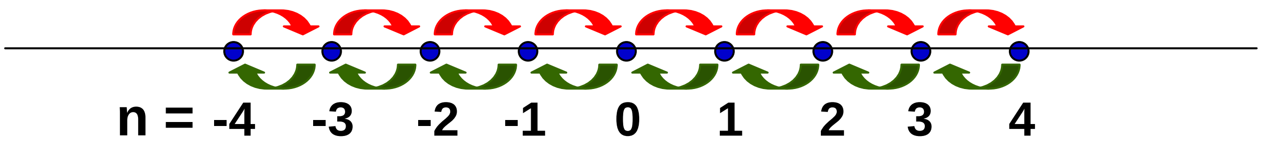

n = number of Cooper pairs on the electrodes

"position" : n, "wave vector" : φ

Cooper pair tunneling $T = -\frac{E_J}{2}\sum_{n=-\infty}^{n=+\infty}\left[|n+1\rangle\langle n| + |n\rangle\langle n+1|\right]$

Plane wave eigenstate: $|\varphi\rangle = \sum_{n=-\infty}^{n=+\infty}|n\rangle$

$$T|\varphi\rangle = -\frac{E_J}{2}\sum_{n'=-\infty}^{n'=+\infty}\left[|n'+1\rangle\langle n'| + |n'\rangle\langle n'+1|\right]\sum_{n=-\infty}^{n=+\infty}e^{i\varphi n}|n\rangle$$

Josephson junction

$$T\left|\varphi\right\rangle = -\frac{E_J}{2}\sum_{n'=-\infty}^{n'=+\infty}\left[\left|n'+1\right\rangle\left\langle n'\right| + \left|n'\right\rangle\left\langle n'+1\right|\right]\sum_{n=-\infty}^{n=+\infty} e^{i\varphi n}\left|n\right\rangle$$

$$= -\frac{E_J}{2}\sum_{n=-\infty}^{n=+\infty} e^{i\varphi n}\left[\left|n+1\right\rangle + \left|n-1\right\rangle\right]$$

$$= -E_J\cos(\varphi)\left|\varphi\right\rangle$$

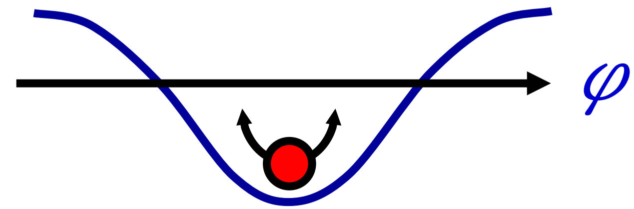

"position" : n, "momentum" : $\hbar\varphi$

Wave packet group velocity

$$\frac{dn}{dt} = \frac{1}{\hbar}\frac{dT}{d\varphi} = \frac{E_J}{\hbar}\sin\varphi$$

Cooper pair tunneling

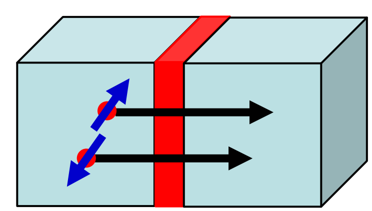

Current

$$I = 2e\frac{dn}{dt} = \frac{2e}{\hbar}E_J\sin\varphi = I_C\sin\varphi$$

Charging energy

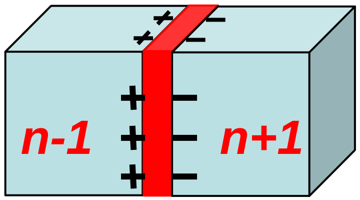

$E_C \equiv 4e^2/2C_\Sigma$

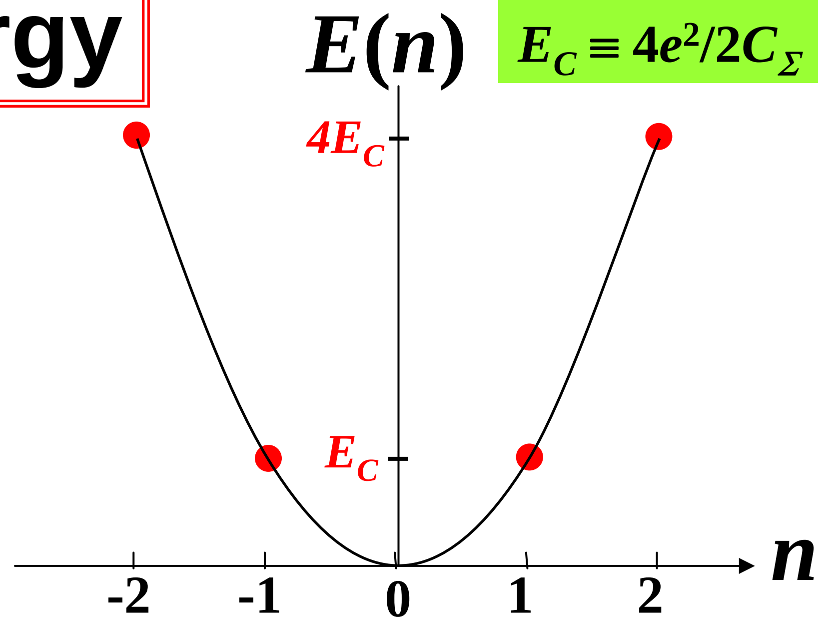

$$|\varphi\rangle = \sum_{n=-\infty}^{n=+\infty} |n\rangle$$

Quantum mechanical conjugate variables: $[n,\ \varphi] = i$

number operator: $\hat{n} \equiv -i \dfrac{\partial}{\partial \varphi}$

φ as coordinate :

$$H = 4E_C \hat{n}^2 - E_J \cos(\varphi)$$
$$= -4E_C \frac{\partial^2}{\partial \varphi^2} - E_J \cos(\varphi)$$

For small phase φ fluctuations:

strong fluctuations in $n \rightarrow$ small E_C

$$H = -4E_C \frac{\partial^2}{\partial \varphi^2} - E_J \cos(\varphi)$$
$$\approx -4E_C \frac{\partial^2}{\partial \varphi^2} - E_J \left[1 - \frac{\varphi^2}{2}\right]$$

note: $p \rightarrow -i\hbar \frac{\partial}{\partial \varphi}$

in φ coordinate

Equivalent to a simple harmonic oscillator with

mass $m = \frac{1}{\hbar^2 8E_C}$

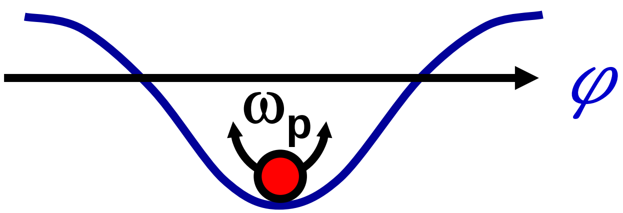

spring constant $K = E_J$

Plasma frequency $\hbar\omega_P = \sqrt{8E_C E_J}$

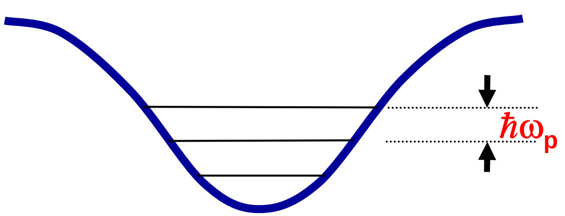

Superconducting charge box

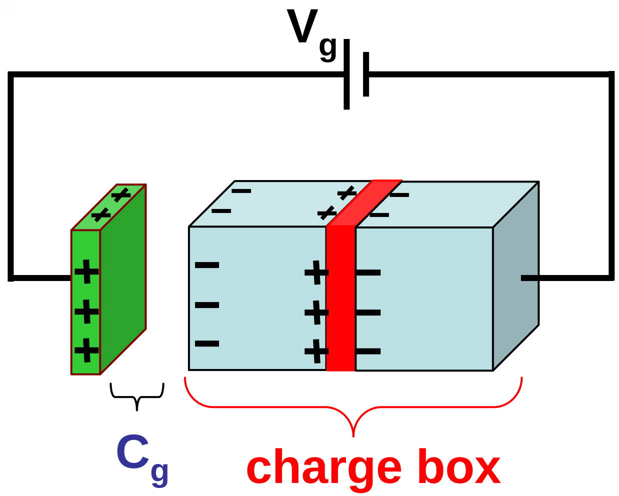

$$H = 4E_C(\hat{n} - n_g)^2 - E_J \cos(\varphi)$$

$n_g = C_g V_g$ is controlled by the gate

V_g=0, charge degenerate

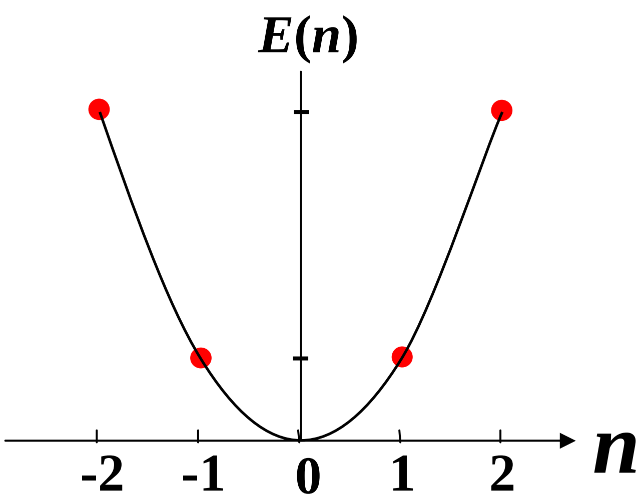

V_g>0, degenerate is lifted

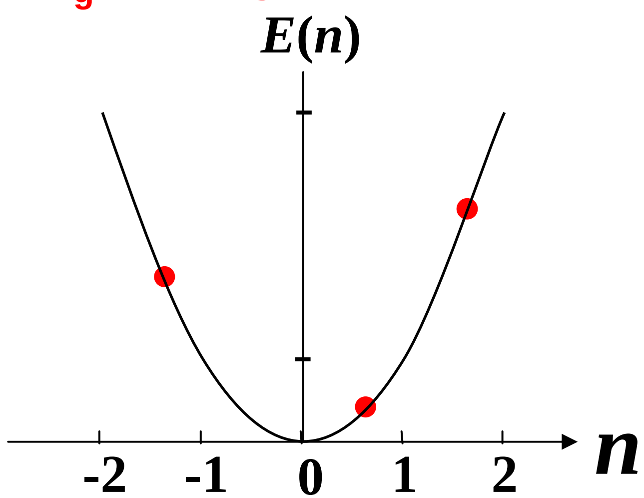

Mapping to two level system

$$H = 4E_C(\hat{n} - n_g)^2 - E_J\cos(\varphi)$$

In ket presentation

$$H = \sum_{n=-\infty}^{n=+\infty} 4E_C(\hat{n} - n_g)^2 |n\rangle\langle n| - \frac{E_J}{2}\left[|n+1\rangle\langle n| + |n\rangle\langle n+1|\right]$$

Assume 1. $E_J \ll E_C$, 2. small n_g, so that only two states $|0\rangle$ and $|1\rangle$ matters

$$H = 4E_C(\frac{1}{2} - C_g V_g)^2 \begin{pmatrix} -1 & 0 \\ 0 & 1 \end{pmatrix} - \frac{E_J}{2}\begin{pmatrix} 0 & 1 \\ 1 & 0 \end{pmatrix}$$

$$= \frac{1}{2}E_{ch}(V_g)\sigma_Z - \frac{1}{2}E_J(B)\sigma_x$$

$$= \frac{1}{2}\begin{pmatrix} +E_{ch} & -E_J \\ -E_J & +E_{ch} \end{pmatrix}$$

$$|\Psi\rangle = \alpha|0\rangle + \beta|1\rangle = \begin{pmatrix} \alpha \\ \beta \end{pmatrix}$$

α and β are complex numbers

$$|0\rangle = \begin{pmatrix} 1 \\ 0 \end{pmatrix}, \quad |1\rangle = \begin{pmatrix} 0 \\ 1 \end{pmatrix}$$

Analogy to a single spin in a magnetic field
Shnirman, Makhlin, Schön, PRL,RMP,Nature

Superposition of the two classical levels

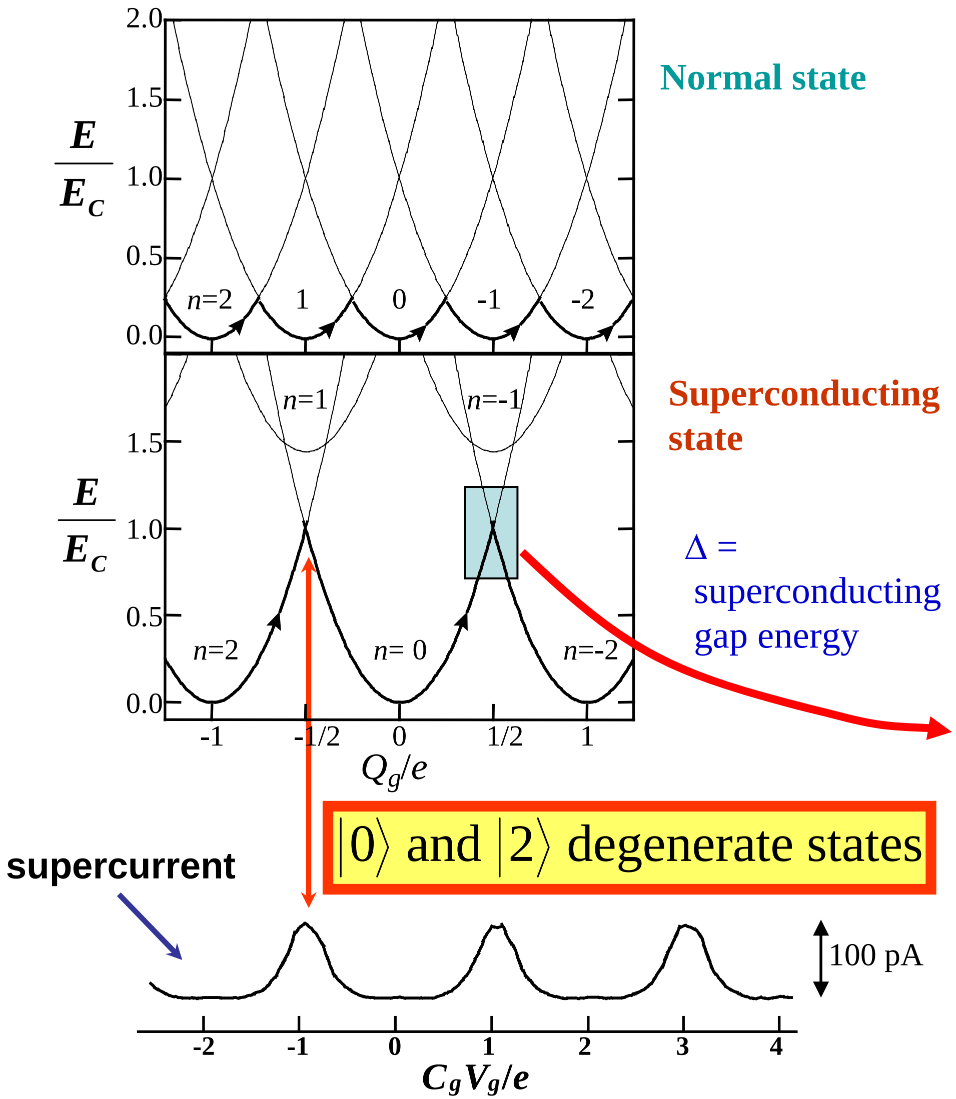

$$H = \frac{1}{2}\begin{pmatrix} +E_{ch} & -E_J \\ -E_J & +E_{ch} \end{pmatrix}$$

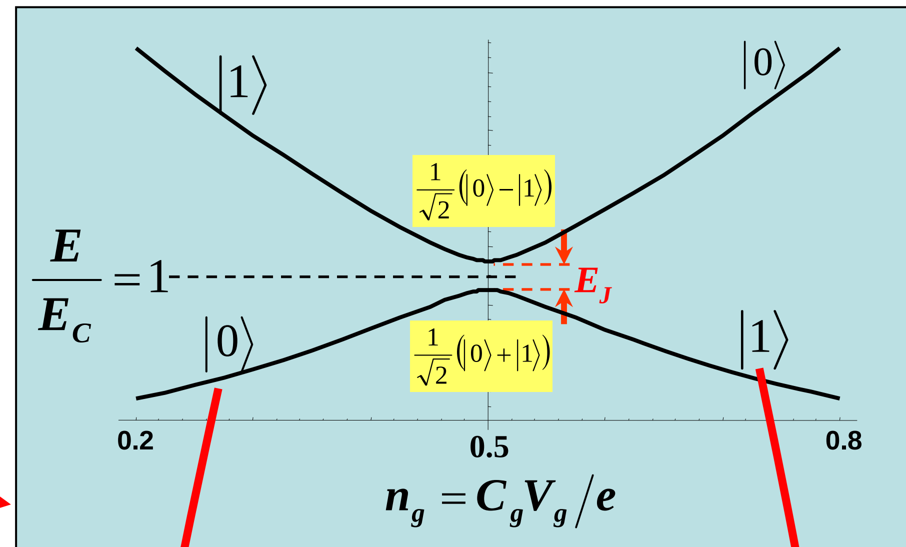

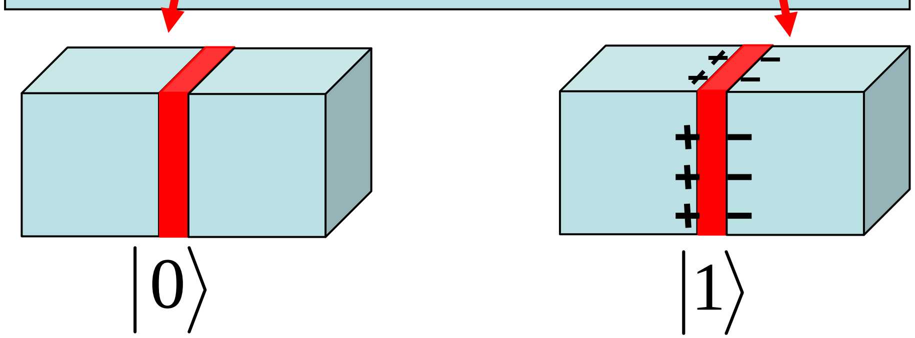

Josephson junction as a diatomic molecule

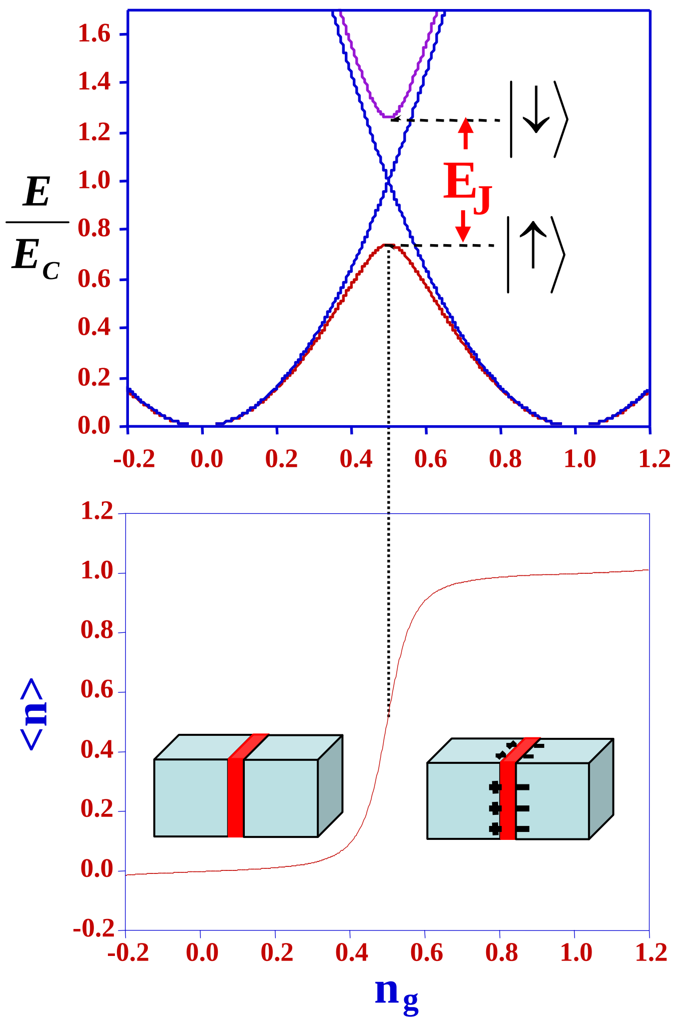

Bonding state

$$|\uparrow\rangle \equiv |\Psi_+\rangle = \frac{1}{\sqrt{2}}\left(|0\rangle + |1\rangle\right)$$

Anti-Bonding state

$$|\downarrow\rangle \equiv |\Psi_-\rangle = \frac{1}{\sqrt{2}}\left(|0\rangle - |1\rangle\right)$$

$$E_{Anti\text{-}Bonding} - E_{Bonding} = E_J$$

Tunable Josephson coupling energy

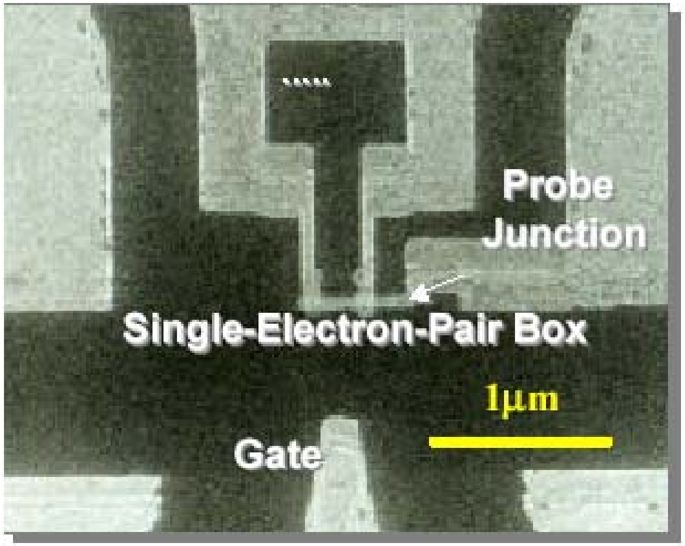

NEC group

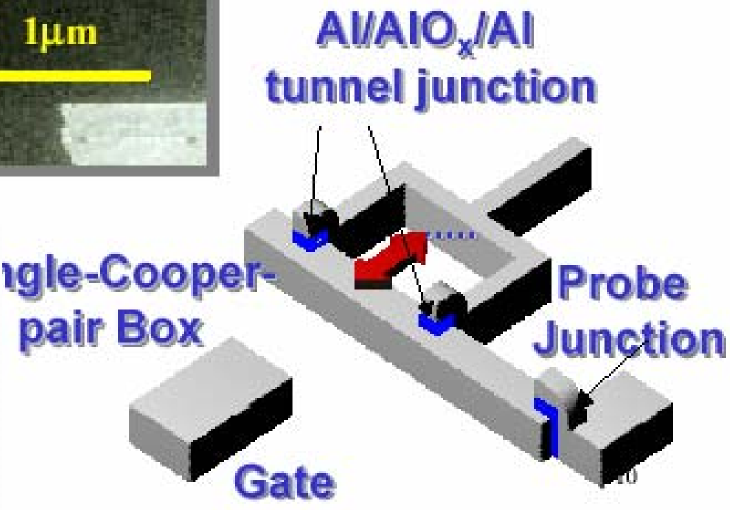

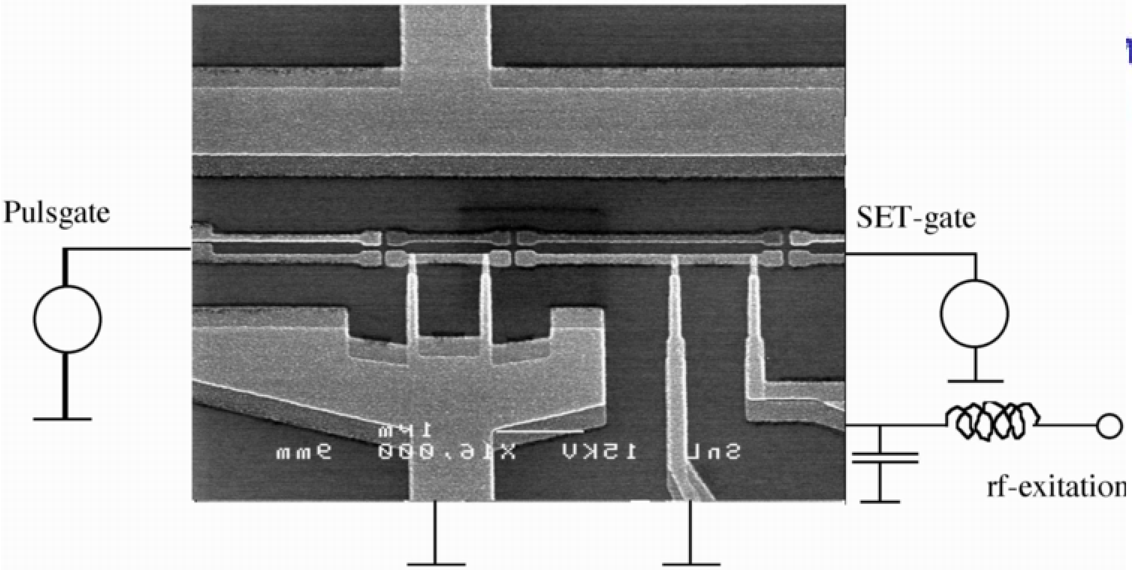

Chalmers group

$$E_J^* = E_J \cos(\Phi)$$

$\Phi = B \cdot A$

A=SQUID loop area

Readout scheme 1 : RF-SET, tank circuit

Chalmers Group

PRL, 86, 3376 (01)

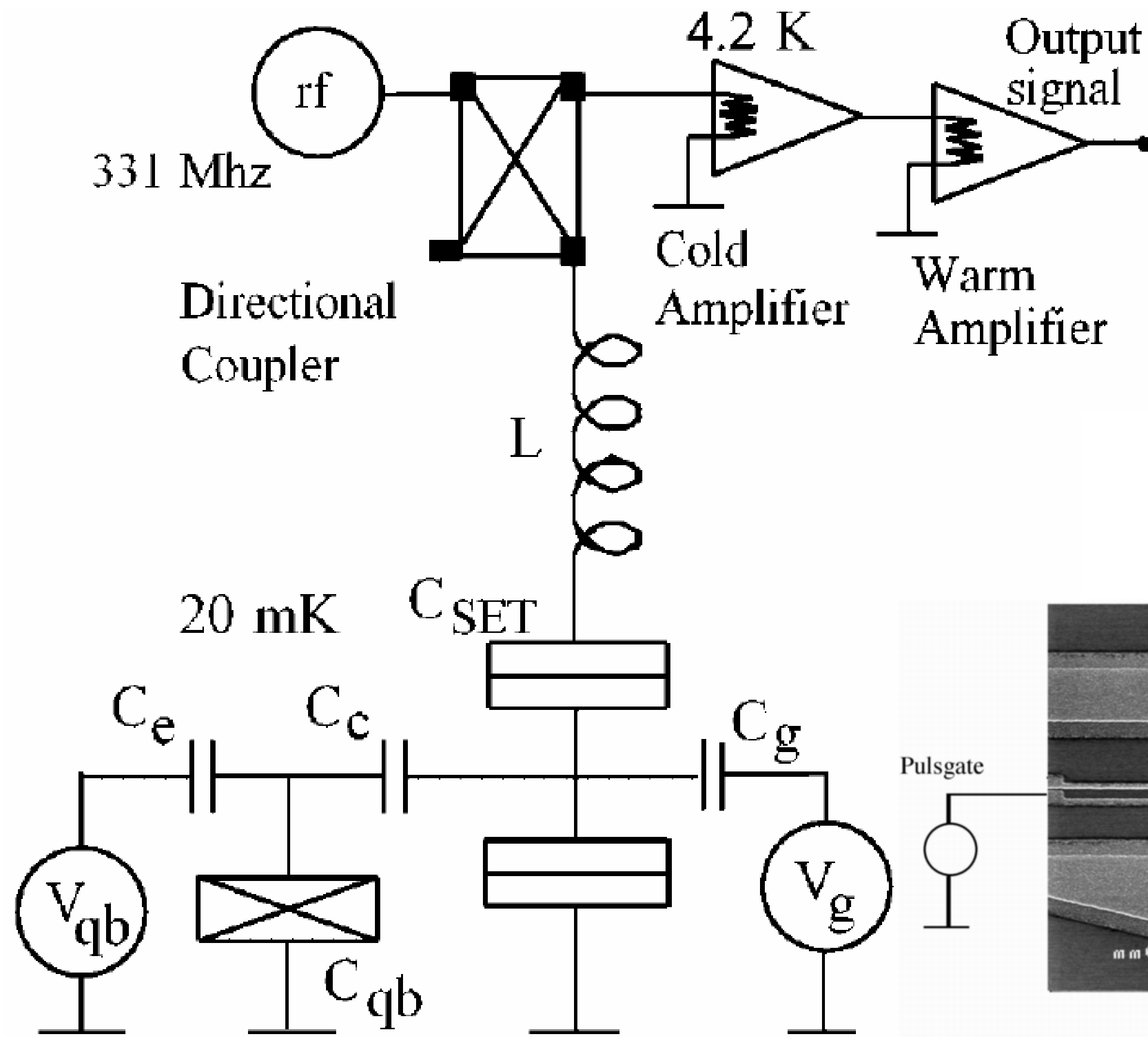

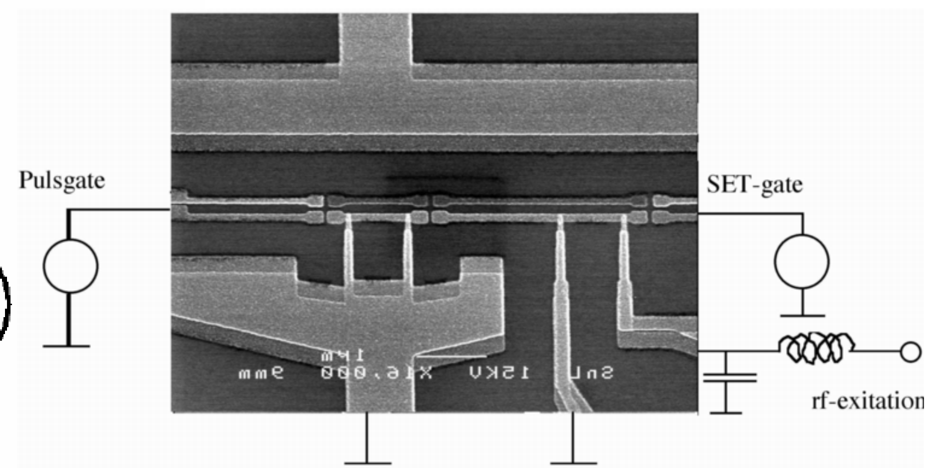

Spectroscopy of **Energy-Level Splitting** between **Two Macroscopic Quantum States** of Charge Coherently Superposed by Josephson Coupling

Y. Nakamura, C. D. Chen, and J. S. Tsai
PRL, 79, 2328 (1997)

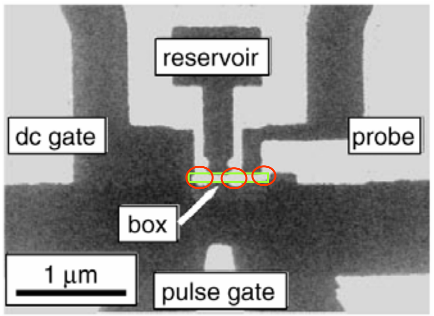

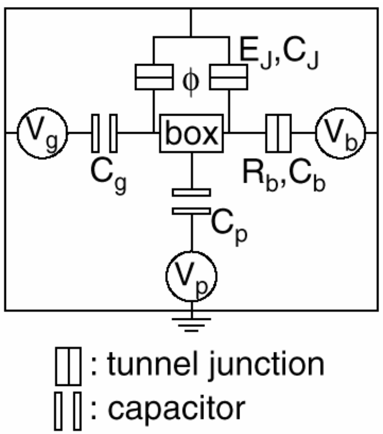

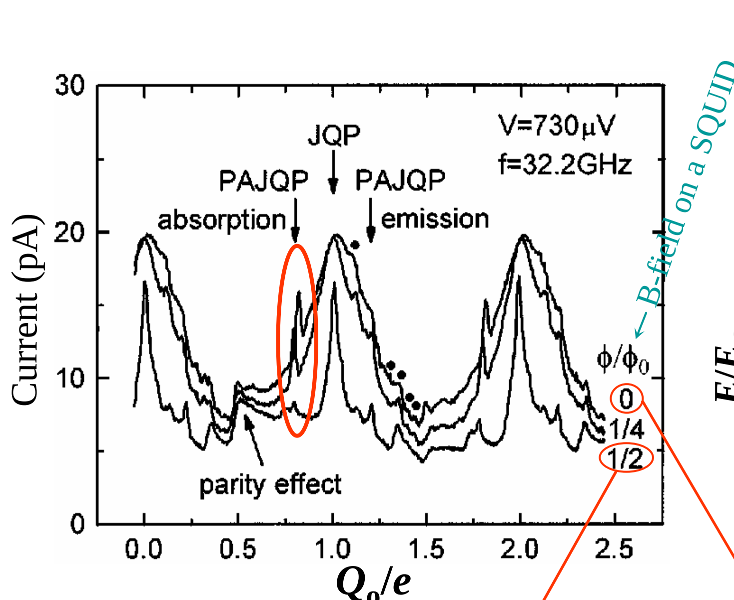

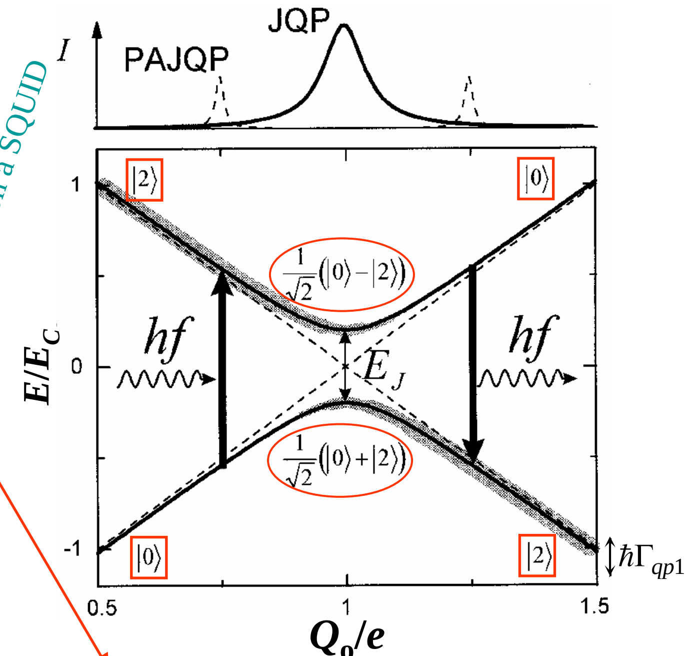

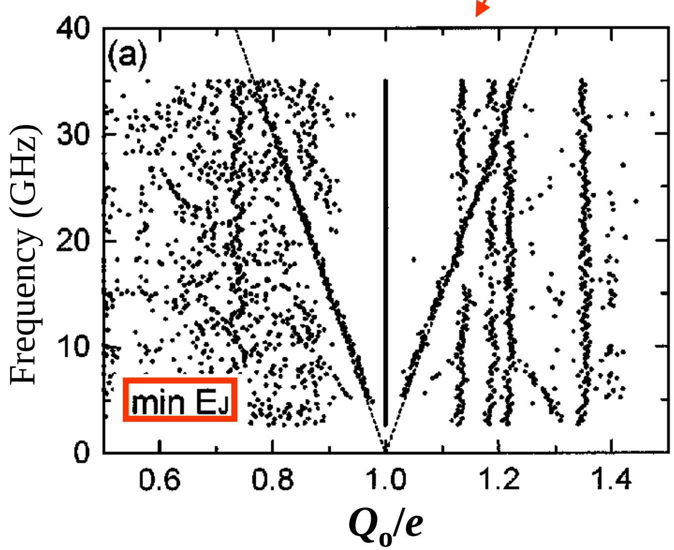

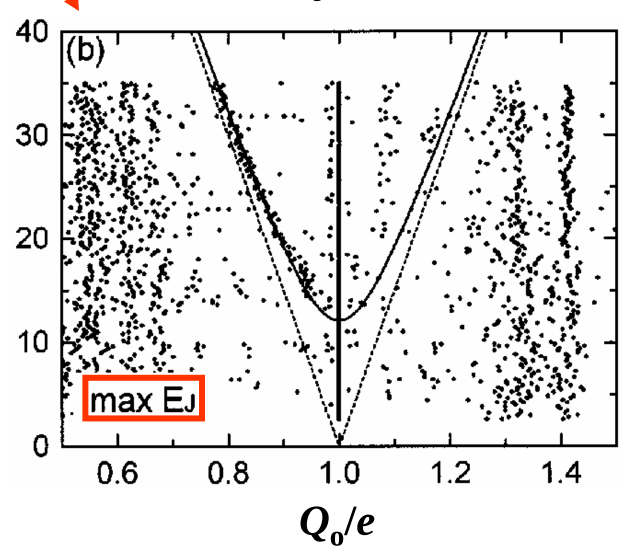

Spin representation:

$$H = -\frac{1}{2}E_{ch}(V_g)\sigma_Z - \frac{1}{2}E_J(B)\sigma_x = \vec{s}\cdot\vec{h}$$

Pauli matrices:

$$\sigma_x = \begin{pmatrix} 0 & 1 \\ 1 & 0 \end{pmatrix} \qquad \sigma_z = \begin{pmatrix} -1 & 0 \\ 0 & 1 \end{pmatrix}$$

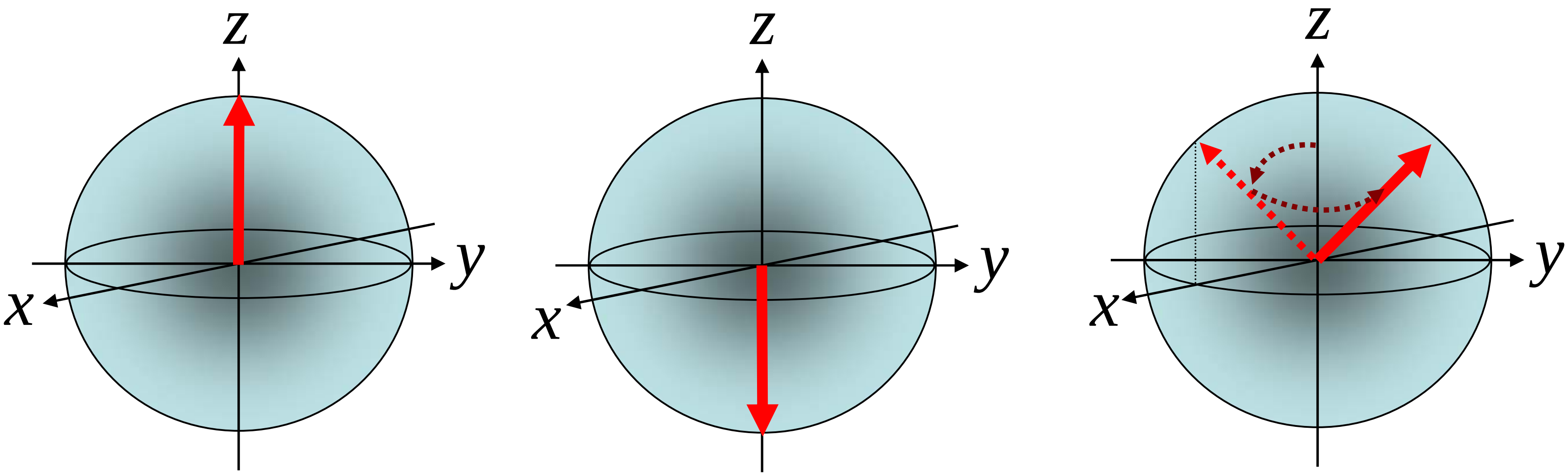

T_1

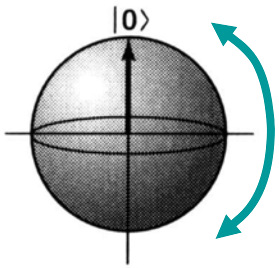

T_2

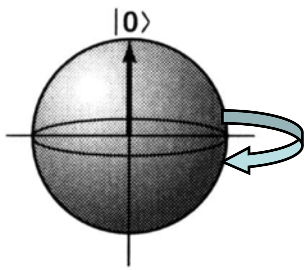

Coherent control of macroscopic quantum states in a single-Cooper-pair box coherent evolution

Y. Nakamura, Yu. A. Pashkin & J. S. Tsai

Nature, v. 398, p. 386, Apr, 1999

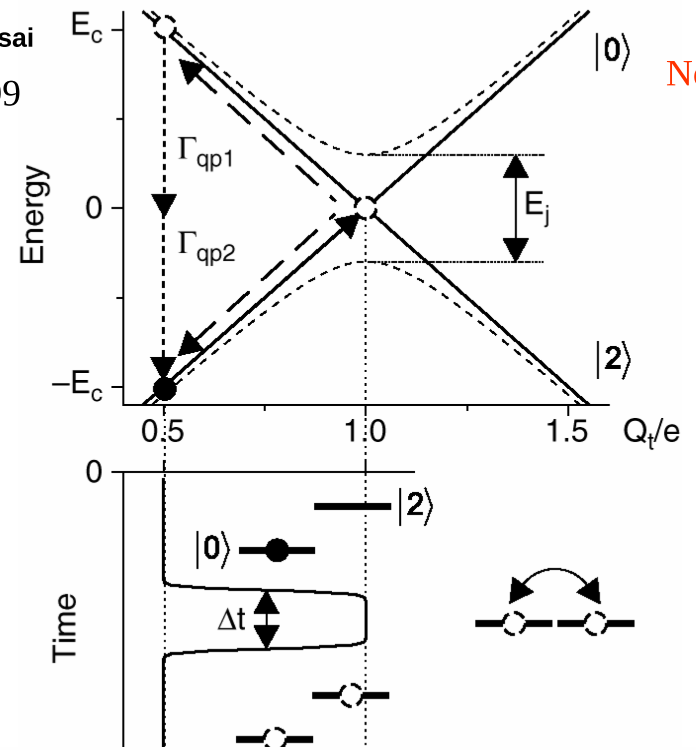

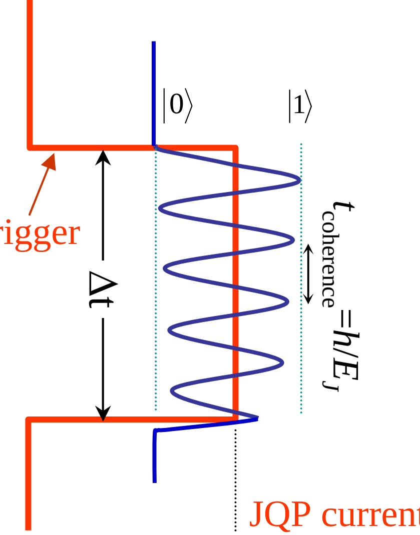

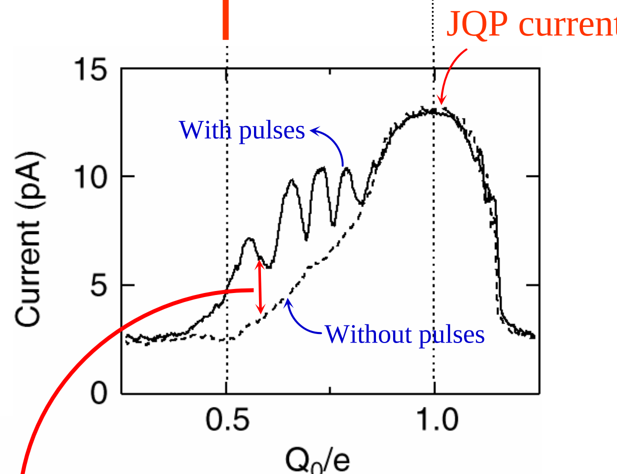

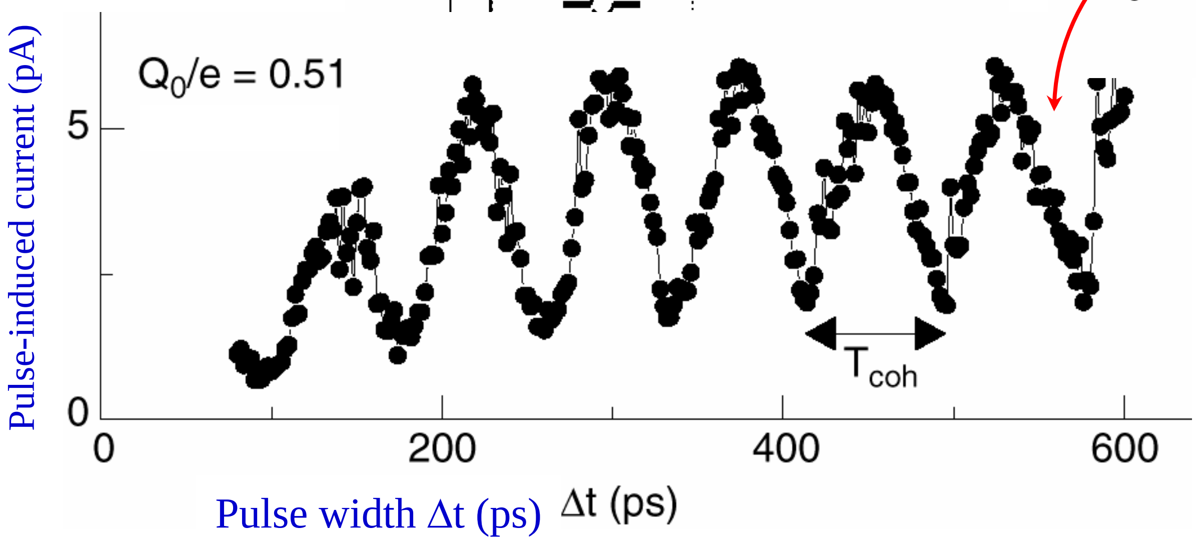

Decoherence:

$\hbar \approx 0.658\times10^{-15}$ eV-s $\approx$ 1nV acting on an electron for 1μs

Possible sources of decoherence:

- **Back ground charges** are known as an important source of decoherence. At the degeneracy point, that decoherence should be drastically reduced. However, if the dc-pulse is not perfectly square, the system is not exactly at the degeneracy point during the evolution. Then background charge noise couples stronger to the system.
- **The SET: The continuous measurement** can of course decohere the system, pulsed measurements should improve the situation.
- **Non-equilibrium quasi particles** may be present in the system. Transition between exited state and qp state
- **DC-pulses** may shake up background charges or other resonant modes (environment, cavity etc.).

Thank you and wish you

a Merry Christmas
and
a prosperous 2009